

# Interactions Between Fast and Slow Dynamics in Nonlinear Evolution Equations

JKT

October 2018

# Contents

<b>1 MATLAB Stuff</b>	<b>1</b>
<b>2 Fast-Slow Systems</b>	<b>1</b>
<b>3 Geometric Singular Perturbation Theory</b>	<b>2</b>
<b>4 Singularities and Fold Points</b>	<b>4</b>
<b>5 The Van Der Pol Equation</b>	<b>5</b>
5.1 Derivation of the Van der Pol Fast-Slow System . . . . .	5
5.2 Phase Plane Analysis . . . . .	6
5.3 Transformation of the Van der Pol System . . . . .	7
5.4 Reduced Dynamics . . . . .	8
5.5 Canonical Form . . . . .	8
5.6 Extended System . . . . .	8
<b>6 The Blow-Up Method</b>	<b>9</b>
6.1 Coordinate Transformation and Charts . . . . .	10
6.2 Dynamics in $K_2$ . . . . .	11
6.3 Dynamics in $K_1$ . . . . .	13
6.4 Dynamics in $K_3$ . . . . .	17
6.5 The Full Solution . . . . .	20
<b>7 Canard Points</b>	<b>20</b>
7.1 Canard Blow-up . . . . .	23
7.1.1 Dynamics in $K_2$ . . . . .	24
7.1.2 Dynamics in $K_1$ . . . . .	26
7.2 Effect of the Canard Point . . . . .	27
7.2.1 Singular Hopf Bifurcation . . . . .	28
7.2.2 Separation of the Manifolds . . . . .	29
<b>8 Folded Singularities in a Three Dimensional System</b>	<b>30</b>
<b>9 MMO</b>	<b>34</b>
9.1 Oscillations . . . . .	34
9.2 Folded Nodes . . . . .	34
9.3 Singular Hopf Bifurcation . . . . .	39
<b>10 Acknowledgements</b>	<b>41</b>
<b>A Elements of Dynamical Systems</b>	<b>43</b>
A.1 Stable Manifold Theorem . . . . .	43
A.2 Centre Manifold Theorem . . . . .	43
A.3 Implicit Function Theorem . . . . .	43
A.4 Hartman Grobman Theorem . . . . .	43

A.5	Hopf Bifurcations . . . . .	43
<b>B</b>	<b>Theorems</b>	<b>43</b>
<b>C</b>	<b>Numerical Simulation</b>	<b>43</b>
C.1	Stiff Solvers . . . . .	45
<b>D</b>	<b>Dynamics in <math>K_2</math></b>	<b>46</b>

## List of Figures

1	Flows in the Van der Pol system. . . . .	2
2	Three charts mapping different sections of our blow up ( <a href="#">Krupa &amp; Szmolyan 2001</a> ). . . . .	10
3	Phase portrait for chart 2 ( <a href="#">Krupa &amp; Szmolyan 2001</a> ) . . . . .	12
4	Riccati solution for chart 2 ( <a href="#">Krupa &amp; Szmolyan 2001</a> ) . . . . .	13
5	Dynamics in chart 1 ( <a href="#">Krupa &amp; Szmolyan 2001</a> ) . . . . .	14
6	Flow on the Van der Pol system. . . . .	20
7	The reduced flow where a) $\lambda = 0$ and b) $\lambda > 0$ . . . . .	21
8	The Van der Pol system for the canard case. . . . .	23
9	The trajectories associated with the canards case of the Van der Pol system. . . . .	28
10	The flow within our canard system ( <a href="#">Krupa &amp; Szmolyan 2001</a> ). . . . .	29
11	Separation of $M_a$ and $M_r$ ( <a href="#">Kuehn 2015</a> ). . . . .	29
12	Three dimensional Van der Pol ( <a href="#">Festschrift et al. 2001</a> ). . . . .	31
13	Phase portraits of our three dimensional system where a) is a folded saddle, b) folded node, c) and d) are desingularised flows ( <a href="#">Desroches et al. 2012</a> ). . . . .	33
14	The branches of a spiral . . . . .	33
15	Numerical Stability Comparison . . . . .	45
16	Stiff Solvers . . . . .	46

### Abstract

This project will be considering the Fast-Slow dynamics in non-linear ordinary differential equations. The project will start by considering the theory associated with Fast-Slow dynamical systems such as Geometric Perturbation Theory (Section 3). Then the project moves onto two-dimensional systems by first looking at the general form, using Krupa & Szmolyan (2001) theory (Section 2), before applying it to the Van der Pol system (Section 5). From here the project will also consider the non-hyperbolicity of the fold points present in the system, where a jump might occur (Section 6). Once the system has been ‘blown-up’ for the normal case, it is prudent to consider the canard system - where the parameter  $\lambda$  is introduced. This could cause a split within the manifolds or a Hopf bifurcation could occur causing a periodic solution (Sections 7 and 7.2.2). Once this has been considered, the next step is to consider the Fast-Slow system in a three dimensional case for folded singularities (Section ??) before continuing onto the theory behind Mixed Mode Oscillations (Section 9.1). **Lastly, the project will discuss the numerical simulations associated with the construction of the models and the results obtained (Section 1).**

## 1 MATLAB Stuff

## 2 Fast-Slow Systems

Fast-Slow systems are systems of differential equations that can be viewed on two different time scales, which are separated by a parameter. These systems are generally of the form

$$\begin{cases} x' = \frac{dx}{dt} = f(x, y, \lambda, \epsilon), \\ y' = \frac{dy}{dt} = \epsilon g(x, y, \lambda, \epsilon), \end{cases} \quad (1)$$

which is known as the fast system. Using a scaling for the time,  $t = \frac{\tau}{\epsilon}$ , we find that this can be rewritten as

$$\begin{cases} \epsilon \dot{x} = \epsilon \frac{dx}{d\tau} = f(x, y, \lambda, \epsilon), \\ \dot{y} = \frac{dy}{d\tau} = g(x, y, \lambda, \epsilon), \end{cases} \quad (2)$$

which is called the slow system.

Here  $x$  is called the fast variable, while  $y$  is the slow variable.  $\lambda$  is a parameter (see Section 7),  $\epsilon$  is the time scale separation parameter and satisfies  $0 < \epsilon \ll 1$ . The functions  $f$  and  $g$  are required to be sufficiently smooth such that we have  $C^{r+1}$  smoothness, where  $r$  is the number of dimensions present. It is generally possible to have three or more time scales, separated by additional parameters, as well as more state-space variables.

In order to analyse systems (1) and (2) using Geometric Singular Perturbation Theory (GSPT), the singular limit  $\epsilon \rightarrow 0$  is considered:

$$\begin{cases} x' = \frac{dx}{dt} = f(x, y, \lambda, \epsilon) \\ y' = 0, \end{cases} \quad (3)$$

which is called the layer problem, and

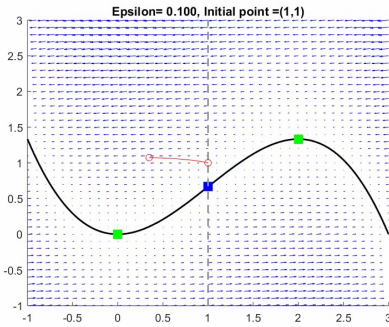
$$\begin{cases} 0 = \epsilon \frac{dx}{d\tau} = f(x, y, \lambda, 0) \\ \dot{y} = \frac{dy}{d\tau} = g(x, y, \lambda, 0), \end{cases} \quad (4)$$

called the reduced system.

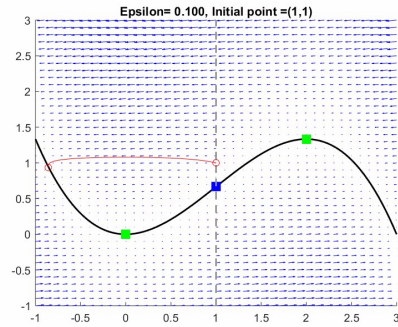
Now considering Equation 4, we can write  $f(x, y, \lambda, 0) = 0$ . Then we are able to define the critical manifold as:

$$S = \{(x, y) : f(x, y, \lambda, 0) = 0\}, \quad (5)$$

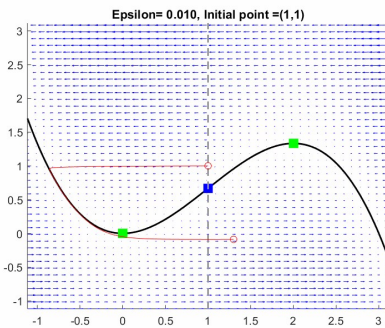
where, by definition of  $S$ , the points  $(x, y) \in S$  are equilibria of (3). Before we continue, it is useful to have a visual interpretation of these flows,



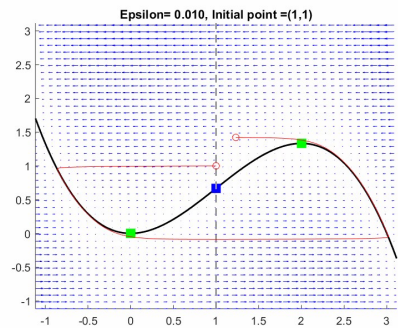
(a) The initial flow within the system starting at  $(x, y) = (1, 1)$ .



(b) The flow as it hits the slow manifold.



(c) The flow as it intersects with the fold point and begins the jump.



(d) The second jump before continuing in a periodic fashion.

Figure 1: Flows in the Van der Pol system.

where we can see that the flows will travel towards our fold point, following the relevant branches. It is worth noting that our flow does not meet the fold point exactly, although this is an ‘error’, it does not directly effect our simulations - as is discussed in Section 1.

### 3 Geometric Singular Perturbation Theory

The main idea of GSPT is the following: Under certain conditions it can be concluded that the critical manifold  $S = S_0$ , where  $\epsilon \rightarrow 0$  persists as an invariant manifold  $S_\epsilon$  under a small perturbation  $\epsilon > 0$ , if  $\epsilon$  is sufficiently small. In higher than 2 dimensions the idea of transversality of the flow of the stable and unstable manifolds is

essential for analysis, while in 2 dimensions this is rather trivial ([Desroches et al. 2012](#)). The main contribution to GSPT comes from Fenichel Theory and his three Theorems can be summed up in one, according to ([Desroches et al. 2012](#)). However, before stating the Theorem, some formal definitions are needed.

**Definition 3.1. Normal Hyperbolicity ([Hek 2009](#))**

A submanifold  $M \subseteq S$  is called normally hyperbolic, if the Jacobian  $\frac{\partial f}{\partial x}(x, y, \lambda, 0)$ , where  $(x, y) \in M$ , has only eigenvalues with nonzero real part.

Moreover, the points  $(x, y) \in M$ ,  $M$  normally hyperbolic, are hyperbolic equilibria of Equation 3 ([Desroches et al. 2012](#)). A normally hyperbolic submanifold can be classified according to its stability property: If  $M$  only has eigenvalues with positive real part it is called repelling, otherwise eigenvalues with negative real part are called attracting and if  $M$  is neither attracting nor repelling it is called a saddle-type submanifold ([Desroches et al. 2012](#)).

Furthermore, stable and unstable manifolds can be defined as  $W^s(M)$  and  $W^u(M)$ , corresponding to the eigenvalues with negative and positive real part, respectively. (???? pretty sure there are two different concepts in the last two sentences.. check needed) Furthermore, with the following definition it is established which notion of distance is going to be employed throughout this analysis.

**Definition 3.2. Hausdorff Distance ([Kuehn 2015](#))**

The Hausdorff Distance of two nonempty sets  $V, W \subset \mathbf{R}^n$ , for some  $n \in \mathbf{N}$  is defined as

$$d_H(V, W) = \max\{\sup_{v \in V} \inf_{w \in W} \|v - w\|, \sup_{w \in W} \inf_{v \in V} \|v - w\|\}.$$

Now combining the above we can state Fenichel's Theorem.

**Theorem 3.3**

**Fenichel's Theorem**

Suppose  $M = M_0$  is a compact, normally hyperbolic submanifold (possibly with boundary) of the critical manifold  $S$  Equation 5 and that  $f, g \in C^r$ ,  $r < \infty$ . Then for  $\epsilon > 0$ , sufficiently small, the following holds:

(F1) There exists a locally invariant manifold  $M_\epsilon$ , diffeomorphic to  $M_0$ . Local invariance means that  $M_\epsilon$  can have boundaries through which trajectories enter or leave.

(F2)  $M_\epsilon$  has a Hausdorff distance of  $O(\epsilon)$  from  $M_0$ .

(F3) The flow on  $M_\epsilon$  converges to the slow flow as  $\epsilon \rightarrow 0$ .

(F4)  $M_\epsilon$  is  $C^r$ -smooth.

(F5)  $M_\epsilon$  is normally hyperbolic and has the same stability properties with respect to the fast variables as  $M_0$  (attracting, repelling or saddle type).

(F6)  $M_\epsilon$  is usually not unique. In regions that remain at a fixed distance from the boundary of  $M_\epsilon$ , all manifolds satisfying (F1)-(F5) lie at a Hausdorff distance  $O(e^{-K/\epsilon})$  from each other for some  $K > 0$  with  $K = O(1)$ .

The normally hyperbolic manifold  $M_0$  has associated local stable and unstable manifolds

$$W^s(M_0) = \cup_{p \in M_0} W^s(p) \quad \text{and} \quad W^u(M_0) = \cup_{p \in M_0} W^u(p),$$

where  $W^s(p)$  and  $W^u(p)$  are the local stable and unstable manifolds of  $p$  as a hyperbolic equilibrium of the layer equations, respectively. These manifolds also persist for  $\epsilon > 0$ , sufficiently small: there exist locally stable and unstable manifolds  $W^s(M_\epsilon)$  and  $W^u(M_\epsilon)$ , respectively, for which conclusions (F1) - (F6) hold if we replace  $M_\epsilon$  and  $M_0$  by  $W^s(M_\epsilon)$  and  $W^s(M_0)$  (or similarly by  $W^u(M_\epsilon)$  and  $W^u(M_0)$ ).

+++direct citation needed for theorem (MMO) +++

Fenichel's Theorem establishes that the submanifold,  $M_0$ , of the critical manifold,  $S_0$ , persists as slow manifold  $M_\epsilon$  as  $\epsilon > 0$ , given it is compact and normally hyperbolic. The theorem furthermore establishes that the stable and unstable manifolds persist as well as the individual fibres, namely  $W^s(p)$  and  $W^u(p)$ , that are associated to each base point  $p \in M_0$ . Therefore, under the assumptions of the theorem, the flow of the Fast-Slow system remains  $O(\epsilon)$  close to the flow of the system in the singular limit  $\epsilon \rightarrow 0$ .

The importance of this result lies in the fact that the behaviour of the full system can be analysed by looking at the system in the singular limit instead, which is often more practical.

+++++also trajectories can be constructed and tested using fenichel... paper 1++++++

## 4 Singularities and Fold Points

One of the requirements of Fenichel's Theorem is normal hyperbolicity ([Kuehn 2015](#)). However, Fast-Slow systems can display singular points where normal hyperbolicity is no longer given and therefore the conclusions of Theorem 3.3 no longer hold at these singularities. The singularities in the setting of Fast-Slow systems are points  $(x_0, y_0)$  on the critical manifold  $S_0$ , for which the Jacobian ( $J$  at  $\partial x(x_0, y_0, \lambda, 0)$ ) has one or more eigenvalue with zero real part. Comparing this with Definition 3.1 shows that this is a negation of normal hyperbolicity. Singularities are points where trajectories can jump between fast and slow flow.

The simplest of those singularities is called a fold point, which is defined as follows:

### Definition 4.1. Fold Point

A fold point  $(x_0, y_0) \in S_0$  is a point where the Jacobian  $\frac{\partial f}{\partial x}(x_0, y_0, \lambda, 0)$  has only one eigenvalue with zero real part.

At the fold point, the system 3 undergoes a saddle-node bifurcation. (+++explain?++) The fold point is non-degenerate if it satisfies the non-degeneracy assumptions:

$$\begin{cases} \frac{\partial^2 f}{\partial x^2}(x_0, y_0, \lambda, 0) \neq 0 \\ \frac{\partial f}{\partial y}(x_0, y_0, \lambda, 0) \neq 0. \end{cases} \quad (6)$$

Furthermore, if  $(x_0, y_0)$  satisfies the transversality condition  $g(x_0, y_0, \lambda, 0) \neq 0$ , then it is called a generic fold point. For these generic folds there exists a theorem that states that the slow flow on  $S_\epsilon$  (?) near  $(x_0, y_0)$  has either positive or negative sign, implying that no equilibria of the slow flow are close to  $(x_0, y_0)$ . Therefore, for generic fold points no canards will be observed, which is a relevant observation for Section 7. To analyse the fold points we need to use a new method called the Blow Up Method, which is discussed in Section 6.

Furthermore, in systems containing generic fold point a certain behaviour of the flow can be observed, called Relaxation Oscillations. These are defined as follows:

### Definition 4.2. Relaxation Oscillation

A periodic trajectory  $\gamma_\epsilon$  is the relaxation oscillation of the Fast-Slow system if the following holds: In the singular limit there exists a trajectory  $\gamma_0$ , which alternates between fast and slow bits and describes a closed loop in the system. This trajectory  $\gamma_0$  persists as  $\gamma_\epsilon$  under a small perturbation  $\epsilon > 0$ .

Systems containing non-generic folds or other types of singularities can display different types of periodic orbits.

## 5 The Van Der Pol Equation

One fast-slow system that contains generic fold points and therefore displays relaxation oscillations is called the Van der Pol System. This can be derived from the Van der Pol Oscillator, which is a well-studied second order ODE that is used to model a variety of physical and biological phenomena. It was developed by the Dutch physicist and electrical engineer Balthasar Van der Pol, who conducted research on electrical circuits, in which he observed stable oscillations, later named relaxation oscillations. The derivation of the Van der Pol Fast-Slow system is presented in the following section, in the form shown in Equation 1.

### 5.1 Derivation of the Van der Pol Fast-Slow System

The Van der Pol Oscillator describes the evolution of the position coordinate  $x(t)$  according to the following ODE:

$$\ddot{x}(t) - \mu(1 - x^2(t))\dot{x}(t) + x(t) = 0, \quad (7)$$

where  $\mu \gg 1$  is a scalar constant.

A new variable  $w = \dot{x} + \mu F(x)$  is introduced, where  $F(x) = \frac{x^3}{3} - x$ .  $F$  is chosen such that  $F'(x) = -(1 - x^2)$  is the nonlinear term in Equation 7. Differentiating  $w$  we obtain

$$\begin{aligned} \dot{w} &= \ddot{x} + \mu \frac{d}{dx} \left( \frac{x^3}{3} - x \right) \frac{dx}{dt} \\ &= \ddot{x} + \mu(x^2 - 1)\dot{x} \\ &= -x \end{aligned}$$

Here, the last equality follows from rearranging Equation 7. We now have a two dimensional system:

$$\begin{cases} \dot{x} = w - \mu F(x) \\ \dot{w} = -x \end{cases}$$

and letting  $y = \frac{w}{\mu}$  results in

$$\begin{cases} \dot{x} = \mu(y - F(x)) \\ \dot{y} = -\frac{x}{\mu}. \end{cases}$$

Now, using a rescaling of time  $\tilde{t} = \mu\tau$  and setting  $\frac{1}{\mu^2} = \epsilon$  results in the system:

+++ $\tilde{t}$  is the original variable, we transform into the slow system but state the fast system first because that's the order we always have them in. slightly confusing. ideas? Also. Need to define  $\lambda$  as either zero or 1 depending on where to mention it...++++++

$$\begin{cases} x' = y - \frac{x^3}{3} + x \\ y' = -\epsilon x, \end{cases} \quad (8)$$

which is of the form (1), the fast system, and the rescaling of time  $t = \epsilon\tau$  results in

$$\begin{cases} \epsilon\dot{x} = y - \frac{x^3}{3} + x \\ \dot{y} = -x, \end{cases} \quad (9)$$

which is in the form of Equation 2, the slow system.

As in Section 2 the fast and slow system can be analysed by considering the limiting case  $\epsilon \rightarrow 0$ . The two systems then become,

$$\begin{cases} x' = y - \frac{x^3}{3} + x, \\ y' = 0, \end{cases} \quad (10)$$

which is of the form (3), the layer problem, and the reduced problem

$$\begin{cases} 0 = y - \frac{x^3}{3} + x := f, \\ \dot{y} = -x. \end{cases} \quad (11)$$

## 5.2 Phase Plane Analysis

Considering Equation 10, it can be observed that the flow is dominated by the dynamics in  $x$  which is cubically depending on  $x$ . Furthermore, it is clear that in the layer problem the dynamics in  $y$  are constant and therefore the flow is horizontal and is only influenced by  $y$  as a constant parameter. Then  $x$  is called the fast variable. This is immediately obvious when comparing this to the reduced problem (11), where the flow is restricted to  $f = 0$ , which is in the form of a cubic function. This defines a critical manifold. Restricted to this manifold, the flow is dominated by the dynamics in  $y$ , which linearly depends on  $x$ , which is much slower than the cubic dependence in the layer problem. Therefore, this is called the slow flow and  $y$  is the slow variable.

The aim of this analysis is to be able to analyse the system in the singular limit  $\epsilon \rightarrow 0$  and apply appropriate theory to conclude the persistence of the dynamic for  $\epsilon > 0$ . Section 3 introduced one instance where this persistence can be concluded. The main requirement for the theory in Section 3 is normal hyperbolicity of the critical manifold. Considering the manifold  $C_0 = \{(x, y) : 0 = y - \frac{x^3}{3} + x := f\}$ , the Jacobian  $\frac{\partial f}{\partial x}(x, y, 0) = -x^2 + 1$ , which has a zero real part at  $x_0 = \pm 1$ . Together with the corresponding  $y_0$  are singularities of the system. Further analysis has to be done below in order to conclude that they are generic fold points. The points of interest are  $(x_0^+, y_0^+) = (1, -\frac{2}{3})$  and  $(x_0^-, y_0^-) = (-1, \frac{2}{3})$ . By Definition 4.1, there is only one eigenvalue with zero real part at  $(x_0, y_0)$ . Evaluating the Jacobian at each of the points in turn shows:

$$\begin{cases} \frac{\partial f}{\partial x}(x_0^+, y_0^+, 0) = -1^2 + 1 = 0 \\ \frac{\partial f}{\partial x}(x_0^-, y_0^-, 0) = -(-1)^2 + 1 = 0, \end{cases}$$

where each of the zeros are simple. Therefore  $(x_0^+, y_0^+)$  and  $(x_0^-, y_0^-)$  are fold points. These points are nondegenerate if the non-degeneracy assumptions (Equation 6) hold:

$$\begin{cases} \frac{\partial^2 f}{\partial x^2}(x_0^+, y_0^+, \lambda, 0) = -2x_0^+ = -2 \neq 0 \\ \frac{\partial f}{\partial y}(x_0^+, y_0^+, \lambda, 0) = 1 \neq 0, \end{cases}$$

and equivalently for the other fold point

$$\begin{cases} \frac{\partial^2 f}{\partial x^2}(x_0^-, y_0^-, \lambda, 0) = -2x_0^- = 2 \neq 0 \\ \frac{\partial f}{\partial y}(x_0^-, y_0^-, \lambda, 0) = 1 \neq 0. \end{cases}$$

Therefore, the two fold points are non-degenerate. Furthermore, it can be checked if a fold point is generic. It then has to satisfy the transversality condition  $g(x_0, y_0, 0) \neq 0$ . The two fold points considered here are generic,

since

$$\begin{aligned} g(x_0^+, y_0^+, 0) &= -1 \neq 0 \\ g(x_0^-, y_0^-, 0) &= 1 \neq 0. \end{aligned}$$

Now we know that the Van der Pol System displays Relaxation Oscillations and that normal hyperbolicity of the system breaks down at the fold points. Fenichel Theory can be applied for regions that are not in the neighbourhood of the fold points. However, a different approach has to be employed for the analysis of the dynamics around the folds.

In order to analyse a fold point it is convenient to transform the Van der Pol system using a coordinate transformation that satisfies the following:

$$\left\{ \begin{array}{l} (x_0, y_0) = (0, 0) \text{ is a fold point,} \\ \frac{\partial^2 f}{\partial x^2}(0, 0, 0) > 0 \\ \frac{\partial f}{\partial y}(0, 0, 0) < 0 \\ g(0, 0, 0) < 0. \end{array} \right. \quad (12)$$

### 5.3 Transformation of the Van der Pol System

In order to analyse the system at the fold points, one fold point at  $(x_0^+, y_0^+) = (1, -\frac{2}{3})$  is considered, and the further analysis is identical for the second fold point  $(x_0^-, y_0^-)$  with a slightly different coordinate transformation. The aim is to find a coordinate transformation that satisfies the conditions in (12). The proposed transformation is  $(x, y) \rightarrow (1 - \tilde{x}, \tilde{y} - \frac{2}{3})$ , which represents a reflection and a translation of the system such that  $(x_0^+, y_0^+)$  is mapped to  $(0, 0)$ .

Now using the proposed mapping  $(x, y) \rightarrow (1 - \tilde{x}, \tilde{y} - \frac{2}{3})$  we are able to redefine the fast system (Equation 8) in the following way,

$$\left\{ \begin{array}{l} x' = -y + x^2 - \frac{(x)^3}{3} \\ y' = \epsilon(x - 1), \end{array} \right. \quad (13)$$

where the tilde has been dropped on  $x$  and  $y$  for convenience. The slow system (Equation 9) is redefined as

$$\left\{ \begin{array}{l} \epsilon x' = -y + x^2 - \frac{(x)^3}{3}, \\ y' = (x - 1), \end{array} \right. \quad (14)$$

using the normal rescaling of time. These two systems will be used throughout the following analysis of the generic fold point. We should note that we have used the general system (Equations 1) to produce the new system where we have chosen  $\lambda = 1$ .

It is readily checked that the coordinate transformation is correct by evaluating Equation 12 for the transformed system. It is clear to see that  $(x_0, y_0) = (0, 0)$ , and differentiation of  $f$  yields  $\frac{\partial^2 f}{\partial x^2}(0, 0, 0) = 2 > 0$  and  $\frac{\partial f}{\partial y}(0, 0, 0) = -1 < 0$ . Furthermore,  $g(0, 0, 0) = -1 < 0$ . Consequently, the new system of equations possesses the required qualities.

## 5.4 Reduced Dynamics

In order to determine the reduced dynamics on the critical manifold  $S$ , Equation 14, when  $\epsilon \rightarrow 0$ , we consider the following system,

$$\begin{cases} 0 = f(x, y, 0) = -y + x^2 - \frac{x^3}{3} \\ \dot{y} = g(x, y, 0) = 0 \end{cases} \quad (15)$$

which is the reduced problem (Kuehn 2015). The critical manifold is then defined as

$$S = \{(x, y) : f(x, y, 0) = 0\} = \left\{ (x, y) : y = x^2 - \frac{x^3}{3} \right\}, \quad (16)$$

which is an S-shaped curve. Since the flow on  $S$  is determined by  $\dot{y}$ , it can be seen that since the sign of  $g$  is negative in the neighbourhood of the fold point  $(0, 0)$ , the slow flow on  $S$  is directed towards the fold point.

The two fold points  $(x_0^\pm, y_0^\pm)$  coincide with the extrema of the cubic function  $\phi(x) = y = x^2 - \frac{x^3}{3}$ . Then using the chain rule, the second Equation of 15 is (Krupa & Szmolyan 2001),

$$\phi_x(x)\dot{x} = g(x, \phi(x), 0). \quad (17)$$

Rearranging this gives an expression for the dynamics in  $x$  on  $S$ . We find that  $\phi(x) = x^2 - \frac{x^3}{3}$ , where the derivative with respect to  $x$  gives  $\phi_x(x) = 2x - x^2$ . Therefore Equation 17 becomes

$$\dot{x} = \frac{g(x, \phi(x), 0)}{\phi_x(x)} = \frac{x-1}{2x-x^2} = \frac{x-1}{x(2-x)}.$$

This calculation confirms that the fold points at  $x = 0$  and  $x = 2$  are singularities of the reduced system. Therefore, no conclusions about the dynamics of  $x$  can be made at the fold points. Different methods will have to be developed in order to overcome this.

## 5.5 Canonical Form

In order to simplify the analysis below, it is useful to rewrite the dynamical system in canonical form.

$$\begin{aligned} x' &= -y + x^2 - \frac{x^3}{3} = -y + x^2 + h(x) \\ y' &= \epsilon(x-1) \end{aligned} \quad (18)$$

There is ample reasoning for doing this. The canonical form has been studied in great detail, allowing us to make comparisons and to avoid excess computation, as seen in Krupa & Szmolyan (2001) paper on Extending Geometric Singular Perturbation Theory. Note that the first equation has, locally, the shape of the parabola  $y = x^2$ , which reflects the consideration of the fold point  $(0, 0)$ , which is locally the minimum of a parabola.

## 5.6 Extended System

The canonical system (Equation 18) is then extended to three dimensions by considering  $\epsilon' = 0$ .

$$\begin{aligned} x' &= -y + x^2 + h(x) \\ y' &= \epsilon(x-1) \\ \epsilon' &= 0. \end{aligned} \quad (19)$$

Analysing the stability of the three dimensional system, three eigenvalues can be found by considering the Jacobian matrix, in the singular limit  $\epsilon = 0$ :

$$J = \begin{vmatrix} 2x - x^2 & -1 & 0 \\ 0 & 0 & 0 \\ 0 & 0 & 0 \end{vmatrix} \quad (20)$$

This is an upper triangular matrix and hence  $(\lambda_1, \lambda_2, \lambda_3) = \text{tr}(J) = (2x - x^2, 0, 0)$ . Therefore, at the fold points, where  $x = 0$  or  $x = 2$ ,  $\lambda_i = 0$  for  $i = 1, 2, 3$ , there exists a zero eigenvalue on  $S$ . At these points  $S$  is not normally hyperbolic. The critical manifold has to be divided as follows:

$$\begin{aligned} S^a &= \{(x, y) : y = x^2 - \frac{x^3}{3}, x < 0\} \cup \{(x, y) : y = x^2 - \frac{x^3}{3}, x > 2\} \\ S^r &= \{(x, y) : y = x^2 - \frac{x^3}{3}, 0 < x < 2\}, \end{aligned}$$

such that  $S^a \cup S^r \cup \{0\} \cup \{2\} = S$ . The manifolds  $S_0^a$  and  $S_0^r$  are normally hyperbolic everywhere and Fenichel's Theorem (Theorem 3.3) can be applied in order to conclude the persistence of the manifold as slow manifolds  $S_\epsilon^a$  and  $S_\epsilon^r$ . At the points  $\{0\}$  and  $\{2\}$  the normal hyperbolicity is not given, since the eigenvalue associated to  $S$  is zero at these points. ++++++Note: technically the paper mentions here the centre manifold M, stressing the three dimensionality of the problem. if we want that it can be added++++++

The problem that the Van der Pol System provides now is the analysis at the fold points. In the analysis of the reduced system it became apparent that the fold points are singularities of the reduced flow on  $S_0$ , and therefore the dynamics in the singular limit cannot be determined. Furthermore, Fenichel Theory does not apply at the folds because normal hyperbolicity breaks down at these points, as discussed above. Therefore, even if the dynamics around the folds in the singular limit was known, no conclusions could be drawn for the perturbed system with  $S_\epsilon$ . Alternative methods have to be employed to describe the dynamics on the fold points in the singular limit and furthermore to be able to conclude the dynamics of the full system at the fold points from this analysis. The method considered for analysis is called the Blow-Up Method and is considered in the following section.

## 6 The Blow-Up Method

In order to apply the Blow-Up Method to the fold point at the origin, we focus on a neighbourhood  $U$  around the fold point  $(0, 0)$ . The neighbourhood  $U$  is small enough, such that  $g(x, y, \epsilon) \neq 0$  in  $U$ , and we can define sections in  $U$ , as follows:

$$\begin{aligned} \Delta^{in} &= \{(x, \rho^2), x \in I\} \\ \Delta^{out} &= \{(\rho, y), y \in \mathbf{R}\}, \end{aligned}$$

where  $I \subset \mathbf{R}$ . Now  $\Delta^{in}$  is traverse to  $S^a$ , while  $\Delta^{out}$  is traverse to the fast flow. This enables us to monitor the incoming trajectories from the attracting branch of  $S$  and the trajectories leaving  $U$  in the direction of the fast flow. Then a function  $\pi : \Delta^{in} \rightarrow \Delta^{out}$  can be defined, called the transition map, which describes how the trajectories passing through  $\Delta^{in}$  are mapped onto the outgoing flow in  $\Delta^{out}$ . The following theorem describes the behaviour of the flow under  $\pi$  and a sketch of the proof will be given at the end of this section: ++++last statement not precise+++

**Theorem 6.1** (Krupa & Szmolyan 2001)

Under the assumptions made in this section, there exists  $\epsilon_0 > 0$  such that the following assertions hold for  $\epsilon \in (0, \epsilon_0]$ :

1. The manifold  $S_\epsilon^a$  passes through  $\Delta^{out}$  at a point  $(\rho, h(\epsilon))$ , where  $h(\epsilon) = O(\epsilon^{2/3})$ .
2. The transition map  $\pi$  is a contraction with contraction rate  $O(e^{-c/\epsilon})$ , where  $c$  is a positive constant.

This means that the trajectories that enter  $U$  through  $\Delta^{in}$ , will be funneled into a smaller section of  $\Delta^{out}$  and therefore we are guaranteed to observe the trajectories that enter through  $\Delta^{in}$  in  $\Delta^{out}$ .

Now we are in the position to describe the Method of Blow-Up Transformations in the neighbourhood  $U$ .

## 6.1 Coordinate Transformation and Charts

We first need to transform the extended system (19) with respect to the time variable and the space variables. This coordinate transformation is called the Blow-Up Transformation because the degenerate fold point  $(0, 0)$  (eigenvalue 0, refer to extended system) is regarded as a sphere of radius  $r = 0$ . By rescaling the space variables with respect to different weights of  $r$ ,

$$x = \bar{r}\bar{x} \quad (21a)$$

$$y = \bar{r}^2\bar{y} \quad (21b)$$

$$\epsilon = \bar{r}^3\bar{\epsilon}, \quad (21c)$$

we find that we are able to carry out further analysis, as will follow. +++++ If time and space permit, an analysis of the space B and coordinate map would be good... p.291 krupa++++ Instead of analysing the sphere in polar coordinates, which might seem the most obvious choice of method, the rest of this analysis is done using charts, which are introduced in the next section. This method turns out to be a more natural choice for this problem and maximises computational efficiency. In terms of the blown up fold point, a sphere denoted

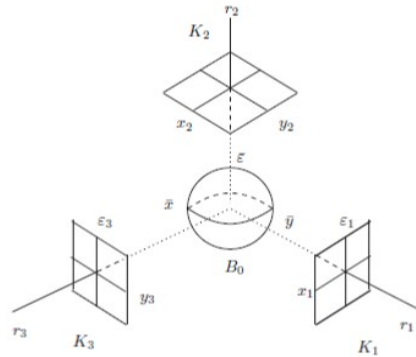


Figure 2: Three charts mapping different sections of our blow up (Krupa & Szmolyan 2001).

by  $B$ , charts are projections of regions of  $B$  onto a two dimensional plane. We introduce three charts  $K_1, K_2$ , and  $K_3$ . Chart  $K_2$  is the two dimensional projection covering the upper half plane of  $B$ . However, as points on the equator of  $B$  are approached on  $K_1$ , the point tends to infinity. These regions however, are of immense interest, since they are points of incoming and outgoing trajectories. As a consequence, charts  $K_1$  and  $K_3$  are introduced, covering the regions of interest on the equator of the fold point. These charts will be discussed in detail in the sections to follow.

The charts are defined by setting each of the variables of the extended system to 1 in turn, giving  $\bar{y} = 1$ ,  $\bar{\epsilon} = 1$ ,  $\bar{x} = 1$ . Substituting these into Equations (21a), (21b) and (21c) respectively gives,

$$x = r_1 x_1, \quad y = r_1^2, \quad \epsilon = r_1^3 \epsilon_1, \quad (22a)$$

$$x = r_2 x_2, \quad y = r_2^2 y_2, \quad \epsilon = r_2^3 \quad (22b)$$

$$x = r_3, \quad y = r_3^2 y_3, \quad \epsilon = r_3^3 \epsilon_3 \quad (22c)$$

where  $(x_i, r_i, \epsilon_i) \in \mathbf{R}^3$  for  $i = 1, 2, 3$ , and the equations correspond to the charts in numerical order (Krupa & Szmolyan 2001). With this setup, we can consider the individual charts in turn, analyse the dynamics on the individual charts, and then join the gathered information into a global view on the dynamics in  $U$ . We start with  $K_2$ , because it holds the most information and the flow is the analysed more readily than in the other two charts. The remaining question is how the transition between the three charts and the connection to the global dynamics is made after finishing the individual analysis. This is done via a coordinate change, derived by using equations (22) and (21), and the results are summed up in the following Lemma:

### Lemma 6.2

Let  $\kappa_{12}$  denote the change of coordinates from  $K_1$  to  $K_2$ . Then  $\kappa_{12}$  is given by

$$x_2 = x_1 \epsilon_1^{-1/3}, \quad y_2 = \epsilon_1^{-2/3}, \quad r_2 = r_1 \epsilon_1^{1/3},$$

for  $\epsilon_1 > 0$ , and  $\kappa_{12}^{-1}$  is given by

$$x_1 = x_2 y_2^{-1/2}, \quad r_1 = r_2 y_2^{1/2}, \quad \epsilon_1 = y_2^{-3/2},$$

for  $y_2 > 0$ . Let  $\kappa_{23}$  denote the change of coordinates from  $K_2$  to  $K_3$ . Then  $\kappa_{23}$  is given by

$$r_3 = r_2 x_2, \quad y_3 = y_2 x_2^{-2}, \quad \epsilon_3 = x_2^{-3},$$

for  $x_2 > 0$ , and  $\kappa_{23}^{-1}$  is given by

$$x_2 = \epsilon_3^{-1/3}, \quad y_2 = y_3 \epsilon_3^{-2/3}, \quad r_2 = r_3 \epsilon_3^{1/3},$$

for  $\epsilon_3 > 0$ .

Furthermore, transition maps  $\Pi_i, i \in 1, 2, 3$  are defined in each section, describing how the trajectories coming in and out of each chart. These are combined in the final part of this section to give the proof of Theorem 6.1, and to relate the results of the blow up method back to the original transition map  $\pi$ .

## 6.2 Dynamics in $K_2$

To be able to consider chart  $K_2$ , the transformation presented in Equation (22b) is applied to the extended system (19). Furthermore, a time rescaling ( $t_2 = r_2 t$ ) is applied to desingularise the system. This results in:

$$\begin{aligned} \frac{d}{dt}(r_2 x_2) &= r_2^2 \frac{dx_2}{dt} = -y_2 + x_2^2 - \frac{x_2^3 r_2}{3}, \\ r_2^3 y'_2 &= r_2^3 (-1 + r_2 x), \\ r'_2 &= 0, \end{aligned} \quad (23)$$

noting that  $\frac{dr}{dt_2} = \frac{dt}{dt_2} \frac{dr}{dt} = \frac{1}{r_2} \frac{dr_2}{dt}$ . Now dividing through by  $r_2^2$  and  $r_2^3$  respectively for each equation and grouping  $O(r_2)$  terms we get,

$$\begin{aligned} x'_2 &= x_2^2 - y_2 + O(r_2), \\ y'_2 &= -1 + O(r_2), \\ r'_2 &= 0. \end{aligned} \quad (24)$$

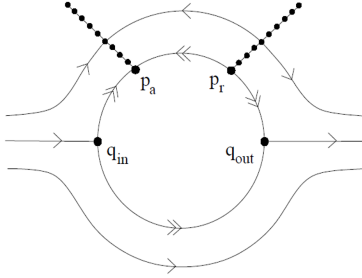


Figure 3: Phase portrait for chart 2 ([Krupa & Szmolyan 2001](#)).

Then, considering  $r_2 = 0$  and neglecting the  $O(r_2)$  terms results in:

$$\begin{aligned} x'_2 &= x_2^2 - y_2, \\ y'_2 &= -1, \end{aligned} \tag{25}$$

which are the well known Riccati equations- see [Mishchenko \(2012\)](#). Some known results about the Riccati equations can be summarised as follows:

**Proposition 6.3** ([Krupa & Szmolyan 2001](#))

*The Riccati equation (25) has the following properties:*

1. Every orbit has a horizontal asymptote  $y = y_r$ , where  $y_r$  depends on the orbit such that  $x \rightarrow \infty$  as  $y$  approaches  $y_r$  from above.
2. There exists a unique orbit  $\gamma_2$ , which can be parameterized as  $(x, s(x))$ ,  $x \in \mathbf{R}$  and is asymptotic to the left branch of the parabola  $x^2 - y = 0$ , for  $x \rightarrow -\infty$ . The orbit  $\gamma_2$  has a horizontal asymptote  $y = -\Omega_0 < 0$ , such that  $x \rightarrow \infty$  as  $y$  approaches  $-\Omega_0$  from above.
3. The function  $s(x)$  has the asymptotic expansions

$$\begin{aligned} s(x) &= x^2 + \frac{1}{2x} + O\left(\frac{1}{x^4}\right), x \rightarrow -\infty, \\ s(x) &= -\Omega_0 + \frac{1}{x} + O\left(\frac{1}{x^3}\right), x \rightarrow \infty. \end{aligned}$$

4. All orbits to the right of  $\gamma_2$  are backward asymptotic to the right branch of the parabola  $x^2 - y = 0$ .
5. All orbits to the left of  $\gamma_2$  have a horizontal asymptote  $y = y_l > y_r$ , where  $y_l$  depends on the orbit, such that  $x \rightarrow -\infty$  as  $y$  approaches  $y_l$  from below.

The solutions to the Riccati equations, described in Proposition 6.3, are displayed in Figure. Note that the equation  $x^2 - y = 0$  is locally the critical manifold  $S$  close to the fold point, under neglegation of  $r_2$  terms.++a bit wavy argument++ The orbit  $\gamma_2$ , corresponds to the global trajectory  $\gamma$ , of the full system, which is the candidate trajectory connecting the slow flow on  $S^a$  entering  $U$  through  $p_a$  to the fast fibres, exiting  $U$  through  $q_{out}$  - described by Figure 4.

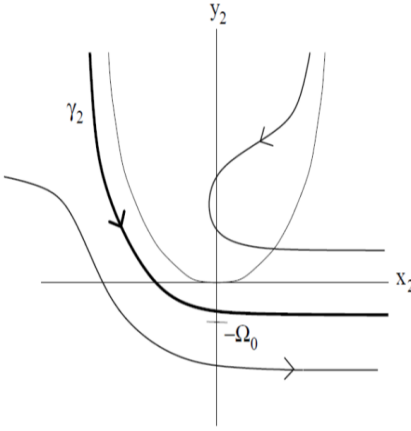


Figure 4: Riccati solution for chart 2 (Krupa & Szmolyan 2001).

This leads to the conclusion that if we can connect  $\gamma_2$  to  $p_a$  through  $K_1$  and to  $q_{out}$  through  $K_3$ , the global  $\gamma$  can be constructed using Lemma 6.2. This motivates the analysis of  $K_1$  and  $K_3$ . In order to connect the dynamics on  $K_2$  to that on the other charts, we need to define local inflow and outflow sections, similar to  $\Delta^{in}$  and  $\Delta^{out}$  in the full system. Then we can follow trajectories that get mapped by  $\Pi_2$ , again analogous to  $\pi$  in the full system, from a section  $\Sigma_2^{in}$  to  $\Sigma_2^{out}$ . The sections are defined as follows. For  $\delta > 0$ , we have:

$$\begin{aligned}\Sigma_2^{in} &= \{(x_2, y_2, r_2) : y_2 = \delta^{-2/3}\}, \\ \Sigma_2^{out} &= \{(x_2, y_2, r_2) : x_2 = \delta^{-1/3}\}.\end{aligned}$$

Then the transition map  $\Pi_2$  can be defined and the results are summarised as follows:

**Proposition 6.4** (Krupa & Szmolyan 2001)

*The transition map  $\Pi_2$  has the following properties:*

1.

$$\Pi_2(q_0) = (\delta^{-1/3}, -\Omega_0 + \delta^{1/3} + O(\delta), 0)$$

2. *A neighbourhood of  $q_0$  is mapped diffeomorphically onto a neighbourhood of  $\Pi_2(q_0)$ .*

This is sufficient information to now consider the dynamics on  $K_1$ .

### 6.3 Dynamics in $K_1$

The coordinate transformation (22a) is applied to the extended system (19), and a rescaling of time,  $t_1 = r_1 t$ , to get

$$\begin{aligned}\frac{d(r_1 x_1)}{dt_1} \frac{dt_1}{dt} &= -r_1^2 + r_1^2 x_1^2 - \frac{1}{3} r_1^3 x_1^3 \\ \frac{dr_1^2}{dt_1} \frac{dt_1}{dt} &= 2r_1^2 r_1' = r_1^3 \epsilon_1 (-1 + r_1 x_1) \\ \frac{d(r_1^3 \epsilon_1)}{dt_1} \frac{dt_1}{dt} &= (3r_1^2 \epsilon_1 + r_1^3 \epsilon_1') r_1 = 0.\end{aligned}$$

Dividing through by  $\frac{dt_1}{dt} = r_1$  and replacing the expressions for  $\epsilon'_1$  and  $r'_1$  with their expressions in terms of the variables, results in the full system in terms of  $K_1$ . Note that the equation for  $\epsilon'$  is found by rearranging the third equation above.

$$\begin{aligned}x'_1 &= -1 + x^2 + \frac{1}{2}x_1\epsilon_1 + \left( -\frac{1}{2}\epsilon_1x_1^2r_1 - \frac{1}{3}x_1^3 \right) \\r'_1 &= \frac{1}{2}r_1\epsilon_1(-1 + r_1x_1) \\\epsilon'_1 &= \frac{3}{2}\epsilon_1^2(1 - r_1x_1),\end{aligned}$$

and grouping terms in  $r_1$  results in the standard form:

$$\begin{aligned}x'_1 &= -1 + x^2 + \frac{1}{2}x_1\epsilon_1 + O(r_1) \\r'_1 &= \frac{1}{2}r_1\epsilon_1(-1 + O(r_1)) \\\epsilon'_1 &= \frac{3}{2}\epsilon_1^2(1 - O(r_1)).\end{aligned}\tag{26}$$

The system (26) has two invariant planes, that are somewhat equivalent to the notion of a nullcline. In an invariant plane, one of the parameters do not change their value and here these are  $r_1 = 0$  and  $\epsilon_1 = 0$ . If we substitute  $r_1 = 0$  or  $\epsilon_1 = 0$  into (26), the  $r_1$  equation, or  $\epsilon_1$  equation respectively, vanishes, and there is only a two dimensional system left to consider. These two subspaces of (26) will be analysed below. Furthermore, the subspace where  $r_1 = 0$  and  $\epsilon_1 = 0$ , is one dimensional, an invariant line, where the subspaces  $r_1 = 0$  and  $\epsilon_1 = 0$  cross. The following analysis is displayed in Figure 5, illustrating the dynamics on  $K_1$ .

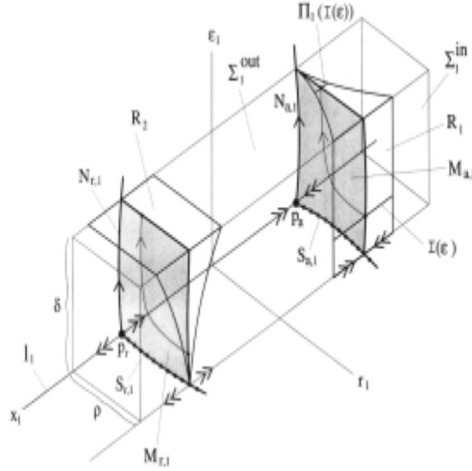


Figure 5: Dynamics in chart 1 ([Krupa & Szmolyan 2001](#))

The invariant line, satisfying  $r_1 = 0$  and  $\epsilon_1 = 0$  is given by  $l_1 = -1 + x^2$ . From this it is easily deduced that the two equilibrium points are where  $l_1 = 0$ , which is at  $x = \pm 1$ . Therefore, the points  $p_a$  and  $p_r$  are defined as  $p_a = (-1, 0, 0)$  and  $p_r = (1, 0, 0)$ . The flow on  $l_1$  is attracted to  $p^a$  and repelled by  $p^r$ , which is easily observed from the form  $l_1$  takes or from a formal stability analysis of the one dimensional system. The eigenvalues of  $l_1$  are found by considering  $l'_1 - \lambda = 2x - \lambda = 0$  which gives that  $\lambda = \pm 2$  at the respective equilibria.

Then we expect the behaviour of the flow on the two invariant planes to be influenced by the two equilibria and the dynamics on  $l_1$ . Consider the plane  $\epsilon_1 = 0$ . The system (Equation 26) becomes

$$\begin{aligned} x'_1 &= -1 + x^2 - \left( \frac{1}{3} r_1 x_1^3 \right) \\ r'_1 &= 0. \end{aligned} \tag{27}$$

This system has equilibria at  $x = \pm 1$ , for  $r_1 = 0$ , as before, however, for each constant value of  $r_1$ , we get a different equilibrium of the system (27). This forms a curve of equilibria, which can be recognise as  $S_1^a$  connected to  $p_a$  and  $S_1^r$ , connected to  $p_r$ , the left and right branches of the critical manifold, transformed into  $K_1$ . This is well illustrated in figure 3. Note. apparently this follows from IFT we got stuck on this before, i cannot remember :(++++++ The additional eigenvalue, corresponding to the  $r_1$  equation, is  $\lambda = 0$ . However, at each of the equilibria of this system, and specifically at  $p_a$  and  $p_r$  we have normal hyperbolicity, due to the coordinate transformation in  $K_1$ . ++ go over this. ++

Next we consider the dynamics on the invariant plane  $r_1 = 0$ . The system (Equation 26) becomes:

$$\begin{aligned} x'_1 &= -1 + x^2 + \frac{1}{2} x_1 \epsilon_1 \\ \epsilon'_1 &= \frac{3}{2} \epsilon_1^2. \end{aligned} \tag{28}$$

Again,  $x = \pm 1$  are equilibria of the system, and an additional zero eigenvalue is gained due to the  $\epsilon$  equation. It can be concluded that one dimensional centre manifolds exist, called  $N_{a,1}$  and  $N_{r,1}$ , that are invariant, however, not manifolds of equilibria like  $S^a$  and  $S^r$  in the  $\epsilon = 0$  plane. The dynamics on these manifolds is determined mainly by the value of  $\epsilon$ , since the change in the  $\epsilon$  direction is much stronger than the change in the  $x$  direction. Therefore, on  $N_{a,1}$  and  $N_{r,1}$  the flow moves up the  $\epsilon$  direction with increasing epsilon.

In order to draw conclusions on the persistence of the dynamics in the full system (+++??+++) **What does this mean?**, as before, sections in the space are defined to monitor incoming and outgoing trajectories. Firstly, let the region considered be such that  $D_1 := \{(x_1, y_1, \epsilon_1) : x_1 \in \mathbf{R}, 0 \leq r_1 \leq \rho, 0 \leq \epsilon_1 \leq \delta\}$ . Then the relevant sections for the candidate trajectory  $\gamma$  are

$$\begin{aligned} \Sigma_1^{in} &:= \{(x_1, r_1, \epsilon_1) \in D_1 : r_1 = \rho\}, \\ \Sigma_1^{out} &:= \{(x_1, r_1, \epsilon_1) \in D_1 : \epsilon_1 = \delta\}. \end{aligned}$$

Note that  $\Sigma_1^{in} = \Delta^{in}$  and  $\Sigma_1^{out} = \Sigma_2^{in}$ . The aim is to find the connection between  $p_a$  and  $\gamma_2$  in  $K_2$ . In order to establish this connection, the trajectory  $\gamma_2$  has to be mapped onto  $K_1$  using Lemma 6.2. Recall from Section 6.2 that the form of the candidate trajectory is of the form  $(x_2, s(x_2))$ . Therefore, the trajectory  $\gamma_1$  satisfies:

$$(x_1, 0, \epsilon_1) = \left( x_2 \left( x_2^2 + \frac{1}{2x_2} + O\left(\frac{1}{x_2^4}\right) \right)^{-1/2}, 0, \left( x_2^2 + \frac{1}{2x_2} + O\left(\frac{1}{x_2^4}\right) \right)^{-3/2} \right).$$

Note that  $s(x_2)$  as  $x_2 \rightarrow -\infty$  is employed, since we consider the left continuation of  $\gamma_2$ . Furthermore, as is intuitively clear from Figure 4, and can be shown by analysing the form of  $\gamma_1$ , the trajectory  $\gamma_1$  converges to

$p_a$  in backward time, which is exactly as expected. This establishes the link between the slow flow on  $S^a$  and the flow on  $K_2$ , if we consider the following proposition, which sums up the findings in  $K_1$  and employs center manifold theory, see Appendix (++++how do i reference that?++++) in order to establish persistence in the full system.

**Proposition 6.5** (Krupa & Szmolyan 2001)

For  $\rho, \delta$  sufficiently small the following assertions hold for the system 26:

1. There exists an attracting two-dimensional  $C^k$ -center manifold  $M_{a,1}$  at  $p_a$  which contains the line of equilibria  $S_1^a$  and the center manifold  $N_{a,1}$ . In  $D_1$  the manifold  $M_{a,1}$  is given as a graph  $x_1 = h_a(r_1, \epsilon_1)$ . The branch of  $N_{a,1}$  in  $r_1 = 0, \epsilon_1 > 0$  is unique.
2. There exists a repelling two-dimensional  $C^k$ -center manifold  $M_{r,1}$  at  $p_r$  which contains the line of equilibria  $S_1^r$  and the center manifold  $N_{r,1}$ . In  $D_1$  the manifold  $M_{r,1}$  is given as a graph  $x_1 = h_r(r_1, \epsilon_1)$ . The branch of  $N_{r,1}$  in  $r_1 = 0, \epsilon_1 > 0$  is not unique.
3. There exists a stable invariant foliation  $F^s$  which base  $M_{a,1}$  and one-dimensional fibres. For any  $c > -2$  there exists a choice of positive  $\rho$  and  $\delta$  such that the contraction along  $F^s$  during a time interval  $[0, T]$  is stronger than  $e^{cT}$ .
4. There exists an unstable invariant foliation  $F^u$  which base  $M_{r,1}$  and one-dimensional fibres. For any  $c > -2$  there exists a choice of positive  $\rho$  and  $\delta$  such that the expansion along  $F^u$  during a time interval  $[0, T]$  is stronger than  $e^{cT}$ .
5. The unique branch  $N_{a,1}$  in  $r_1 = 0, \epsilon_1 > 0$  is equal to  $\gamma_1 := \kappa_{12}^{-1}(\gamma_2)$  wherever  $\kappa_{12}^{-1}(\gamma_2)$  is defined, i.e. along the part of  $\gamma_2$  corresponding to  $y_2 > 0$ .

In order to find the lower bound on the contraction rate along  $F^s$ , the transition time  $T$  has to be found, i.e. the time the trajectory takes to travel from a point  $p = (x_1, \rho, \epsilon_1) \in \Sigma_1^{in}$  to a point in  $\Pi_1(p) = (x_1, r_1, \delta) \in \Sigma_1^{out}$ . This is done by integrating the  $\epsilon$  equation of system (26), which is a separable ODE with respect to  $t_1$ . This then results in

$$T = \frac{2}{3} \left( \frac{1}{\epsilon_1} - \frac{1}{\delta} \right) (1 + O(\rho)),$$

where  $r_1 = \rho \in p$ . Therefore, a transition map  $\Pi_1 : \Sigma_1^{in} \rightarrow \Sigma_1^{out}$  can be defined for small enough parameter values of  $\rho, \delta, \beta_1$  (Why only for small param.?++++++). We are interested specifically in the transition around the center manifolds  $M_{a,1}$  and  $M_{r,1}$ . The following subsections of  $\Sigma_1^{in}$  and  $\Sigma_1^{out}$  can be defined. Let  $R_1 = \{(x_1, \rho, \epsilon_1) : |1 + x_1| \leq \beta_1\}$ , a rectangle in the intersection of the manifolds  $M_{a,1}$  and  $\Sigma_1^{in}$ , and  $R_2 = \{(x_1, r_1, \delta) : |1 - x_1| \leq \beta_1\}$ , a rectangle in the intersection of the manifolds  $M_{r,1}$  and  $\Sigma_1^{out}$ , with  $\beta_1 > 0$  sufficiently small. Furthermore, we can define line segments in these rectangles as  $I_a(\bar{\epsilon}) \subset R_1$  and  $I_r(\bar{r}) \subset R_2$ , where  $0 \leq \bar{\epsilon} \leq \delta$  and  $0 \leq \bar{r} \leq \rho$ . Then for any  $\bar{\epsilon}$ ,  $\Pi_1$  maps the trajectory on a smaller region  $\Pi_1 I_a(\bar{\epsilon}) \in \Sigma_1^{out}$ . This is called a contraction of the trajectories. Considering Theorem 6.1, which states the dependence of the contraction rate on  $\epsilon$ , the bounds on the contraction rate can be related to  $\epsilon$ , the parameter of the original system. Then using the  $K_1$  rescaling of  $\epsilon = \epsilon_1 r_1^3$ , see (22a), the contraction rate for  $\Pi_1|I_r(\bar{r})$  is found by replacing  $\epsilon_1$  by  $\frac{\delta r^3}{\rho^3}$ . Visual understanding of this analysis can be gained by considering Figure 5. ++++ contraction in  $I_r$ ?++ The following proposition summarises the the findings for  $\Pi_1$ :

**Proposition 6.6** (Krupa & Szmolyan 2001)

For  $\rho, \delta$  and  $\beta_1$  sufficiently small, the transition map  $\Pi_1 : \Sigma_1^{in} \rightarrow \Sigma_1^{out}$  defined by the flow of system 26 has the following properties:

1.  $\Pi_1(R_1)$  is a wedge-like region in  $\Sigma_1^{out}$ .  $\Pi_1^{-1}(R_2)$  is a wedge-like region in  $\Sigma_1^{in}$ .
2. More precisely, for fixed  $c < 2$ , there exists a constant  $K$  depending on the constants  $c, \rho, \delta$  and  $\beta_1$  such that
  - (a) for  $\bar{\epsilon} \in (0, \delta]$  the map  $\Pi_1|I_a(\bar{\epsilon})$  is a contraction with contraction rate bounded by  $Ke^{-\frac{2c}{3}(\frac{1}{\bar{\epsilon}} - \frac{1}{\delta})}$ .
  - (b) for  $\bar{r} \in (0, \rho]$  the map  $\Pi_1|I_r(\bar{r})$  is a contraction with cocontraction rate bounded by  $Ke^{-\frac{2c}{3}(\frac{\rho^3}{\bar{r}^3} - \frac{1}{\delta})}$ .

#### 6.4 Dynamics in $K_3$

The final chart to study the behaviour of is  $K_3$ . This chart covers the trajectory as it leaves the fold point at  $q_{out}$ . The other charts could not do this as  $q_{out}$  is close to infinity in both  $K_1$  and  $K_3$  (cf. Figure 2). Similarly to  $K_1$  and  $K_2$ , the system can be analysed using the blow-up transformation (22c).

$$\frac{dr_3}{dt_3} = r_3 F(r_3, y_3, \epsilon_3) \quad (29a)$$

$$\frac{dy_3}{dt_3} = \epsilon_3(r_3 - 1) - 2y_3 F(r_3, y_3, \epsilon_3) \quad (29b)$$

$$\frac{d\epsilon_3}{dt_3} = -3\epsilon_3 F(r_3, y_3, \epsilon_3) \quad (29c)$$

where  $F(r_3, y_3, \epsilon_3) = (1 - y_3 - \frac{r_3}{3})$

Note that as  $\epsilon_3$  and  $r_3$  appear as a factor in their respective derivatives, the planes  $\epsilon_3 = 0$  and  $r_3 = 0$  are invariant and, by extension, so is the  $y_3$  axis.

The aim is to continue the special trajectory found in the other two charts and to find the transition map in and out of this chart. We will then be able to construct a phase portrait for the whole space by combining the dynamics in each chart.

Linearising the system about  $(0, 0, 0) = q_{out}$  gives

$$\begin{pmatrix} \dot{r}_3 \\ \dot{y}_3 \\ \dot{\epsilon}_3 \end{pmatrix} = \begin{pmatrix} 1 & 0 & 0 \\ 0 & -2 & -1 \\ 0 & 0 & -3 \end{pmatrix} \begin{pmatrix} r_3 \\ y_3 \\ \epsilon_3 \end{pmatrix}$$

As the matrix is upper triangular, its eigenvalues are trivially  $\{1, -2, -3\}$  with corresponding eigenvectors  $\{(1, 0, 0), (0, 1, 0), (0, 1, 1)\}$ . This presents an issue as there is additive resonance i.e.  $\lambda_2 - (\lambda_1 + \lambda_3) = 0$ . This means the Poincaré-Dulac theorem does not hold and the vector field is not linearisable, there is no smooth transformation between the nonlinear and linear flow. The nonlinear terms in the expansion will be of the same order as the linear terms, and thus they cannot be disregarded. Despite this, progress can still be made as the form of the equations allow a near identity transformation and yields the lowest order approximation to the flow. Note that  $q_{out}$  is also a hyperbolic equilibrium of the system. +++Mention  $\bar{M}_a$ , the locally invariant perturbation of the center manifold  $M_a$ ? Passes near the delicate equilibrium point  $q_{out}$  so behaviour very much

depends on how we pass this point. +++

The special orbit,  $\gamma_2$ , can be mapped into this chart using the change of coordinates  $\kappa_{23}$  of Equation (6.2).

$$\gamma_3 = \kappa_{23}(\gamma_2)$$

In fact,  $\gamma_3$  lies in the plane  $r_3 = 0$  and converges to  $q_{out}$  as  $\epsilon \rightarrow 0$ . To find the flow in a neighbourhood of  $q_{out}$  we use sections similar to those introduced in  $K_2$ .

$$\begin{aligned}\Sigma_3^{in} &= \{(r_3, y_3, \epsilon_3) : r_3 \in [0, \rho], y_3 \in [-\beta_3, \beta_3], \epsilon_3 = \delta\}, \\ \Sigma_3^{out} &= \{(r_3, y_3, \epsilon_3) : r_3 = \rho, y_3 \in [-\beta_3, \beta_3], \epsilon_3 \in [0, \delta]\}\end{aligned}$$

We now wish to find the transition map  $\Pi_3$  between these two charts. That is, given that the trajectory enters somewhere in  $\Sigma_3^{in}$ , how will it behave until it reaches  $\Sigma_3^{out}$ ? To do this, the system 29 will be studied after some simplification. The system is in fact equivalent to the Riccati equation. Observe that  $F(r_3, y_3, \epsilon_3)|_{q_{out}} = 1 - y_3 + O(r_3)|_{q_{out}} \approx 1$ . Thus dividing (29) through by  $F$  yields

$$\dot{r}_3 = r_3 \tag{30a}$$

$$\dot{y}_3 = -2y_3 - \frac{\epsilon_3}{1 - y_3} + r_3\epsilon_3 G(r_3, y_3, \epsilon_3) \tag{30b}$$

$$\dot{\epsilon}_3 = -3\epsilon_3 \tag{30c}$$

In the invariant plane  $r_3 = 0$ , the system becomes the Riccati equation (cf. (25) transformed into the chart  $K_3$  and with a rescaling of time.

$$\begin{aligned}y'_3 &= -2y_3 - \frac{\epsilon_3}{1 - y_3} \\ \epsilon'_3 &= -3\epsilon_3\end{aligned}$$

This system has eigenvalues  $\{-2, -3\}$  and the issue of additive resonance has been avoided so we are able to linearise the system using a near-identity transformation. This transformation allows the elimination of awkward higher order terms (in this case,  $\frac{1}{1-y_3}$ ). Let

$$y_3 = \psi(\tilde{y}_3, \epsilon_3) = \tilde{y}_3 + O(\tilde{y}_3\epsilon_3).$$

Let  $\tilde{\psi}$  denote the inverse transformation and both be  $C^k$  functions +++? Why, justify+++. The system (30) can now be linearised and the following proposition gives the transition map.

**Proposition 6.7** (Krupa & Szmolyan 2001)

The transition map  $\Pi_3$  for the transformed  $K_3$  system (29) is

$$\Pi_s(r_3, y_3, \delta) = \begin{pmatrix} \rho \\ \Pi_{32}(r_3, y_3, \delta) \\ \left(\frac{r_3}{\rho}\right)^3 \delta \end{pmatrix}$$

where

$$\Pi_{32}(r_3, y_3, \delta) = (\bar{\psi}(y_3, \delta) - \delta) \left(\frac{r_3}{\rho}\right)^2 + O(r_3^3 \ln r_3)$$

*Proof.* We will use the near-identity transformation to find the passage time  $T$  and thus the values of  $r_3, y_3, \epsilon_3$  at this time. For brevity, the subscripts will be omitted for the remainder of this proof. Under the near-identity transformation, system (30) becomes

$$\dot{r} = r, \quad (31a)$$

$$\dot{\tilde{y}} = -2\tilde{y} + \epsilon + r\epsilon H(r, \tilde{y}, \epsilon) \quad (31b)$$

$$\dot{\epsilon} = -3\epsilon \quad (31c)$$

Let the subscript  $i$  denote the value of a variable at its entry into the chart, and likewise  $o$  for out. Then  $(r_i, y_i, \epsilon_i) \in \Sigma^{in}$ , and  $(r_o, y_o, \epsilon_o) \in \Sigma^{out}$ . Thus

$$\begin{aligned} r(0) &= r_i & r(T) &= r_o = \rho \\ y(0) &= y_i & y(T) &= y_o \\ \epsilon(0) &= \epsilon_i = \delta & \epsilon(T) &= \epsilon_o \end{aligned}$$

We wish to construct an equation for the out variables  $(T, \tilde{y}_o, \epsilon_o)$  in terms of the in variables  $(r_i, \tilde{y}_i)$ , that is the transition map. The  $r$  and  $\epsilon$  equations are easily solved:

$$r = r_i e^t \quad \epsilon = \delta e^{-3t} \quad (32)$$

Then using  $r(T) = \rho$ ,

$$r(T) = \rho = r_i e^{-t} \implies T = \ln\left(\frac{\rho}{r_i}\right).$$

For the equation in  $y$ , a little more work is required. We introduce a new coordinate  $z$  as follows,  $\tilde{y} = e^{-2t}(\tilde{y}_i - \delta + z) + \delta e^{-3t}$ . Upon first sight, this seems unlikely to be of any use. However, it turns out that this transformation is ideal as it allows many terms to be removed. First rearrange for  $z$  and differentiate with respect to  $t$ .

$$\begin{aligned} z &= e^{2t}(\tilde{y} - \delta e^{-3t}) - \tilde{y}_i + \delta \\ \frac{dz}{dt} &= 2e^{2t}\tilde{y} + e^{2t}\dot{\tilde{y}} + \delta e^{-t} \end{aligned}$$

Substitute  $\dot{\tilde{y}}$  from Equation (31b) and cancel terms.

$$\begin{aligned} &= e^{2t}(-\epsilon + r\epsilon H(r, \tilde{y}, \epsilon)) + \delta e^{-t} \\ &= -\epsilon e^{2t} + e^{2t}r\epsilon H(r, \tilde{y}, \epsilon) + \delta e^{-t} \\ &= e^{2t}r\epsilon H(r, \tilde{y}, \epsilon) \end{aligned}$$

This final equality follows from the explicit solutions in  $r$  and  $\epsilon$  above. These equations also show that  $r\epsilon e^{2t} = r_i \delta e^{-2t} e^{2t}$ . Finally,

$$\dot{z} = r_i H^z(r_i, \tilde{y}_i, t)$$

where  $H^z$  is the same as  $H$  but under the transformation from  $z$ , i.e.  $H^z(r_i, \tilde{y}_i, t) = \delta H(r_i e^t, e^{-2t}(\tilde{y}_i - \delta + z) + \delta e^{-3t}, \delta e^{-3t})$ . This has not affected the expression for the passage time  $T$ . ++Uniform boundedness of  $H$  implies?++ Hence  $z(T) = r_i O(T) = O(r_i \ln(\frac{\rho}{r_i}))$  Using the initial definition of  $z$ , we recover an expression for  $\tilde{y}(T)$ .

$$\begin{aligned} \tilde{y}(T) &= e^{-2T} \left( \tilde{y}_i - \delta + O\left(r_i \ln\left(\frac{\rho}{r_i}\right)\right) \right) + \delta e^{-3T} \\ &= (\tilde{y}_i - \delta)e^{-2 \ln \frac{\rho}{r_i}} + e^{-2 \ln \frac{\rho}{r_i}} O\left(r_i \ln \frac{\rho}{r_i}\right) + \delta \frac{r_i^3}{\rho^3} \\ &= (\tilde{y}_i - \delta) \frac{r_i^2}{\rho^2} + O\left(\frac{r_i^3}{\rho^2} \ln \frac{\rho}{r_i}\right) \end{aligned}$$

We now have an expression for each of the out variables in terms of the initial conditions, albeit under a near-identity transformation. All that remains is to undo this transformation using the inverse map  $\tilde{\psi}$ .

+++Undo transformation, explain  $r$  and  $\epsilon$  coordinates in prop. ThenDONE!+++ ■

## 6.5 The Full Solution

The analysis of the three charts, discussed in the Sections 6.2-6.4, provided a description of the dynamics on each of the charts, as well as theory to conclude the persistence of the dynamics in the full system. The special trajectory  $\gamma$  has been traced through all charts and in chart 1 it has been linked to the slow flow of  $S^a$ , while in chart 3 the connection to the fast flow has been made. Therefore, the fold point is indeed a jump point, or transition point, which connects the slow and fast dynamic. These transition points can also be seen in the case of singular canards, which are treated in the following section. The remaining issue is the transition of this special trajectory through the charts in order to have a solution of the full system. This is equivalent to finding the transition map  $\pi$  from Theorem 6.1. Let  $\Pi : \Sigma_1^{in} \rightarrow \Sigma_3^{out}$  be the full transition map of the Blow-Up Transformation. Then it satisfies

$$\Pi := \Pi_3 \circ \kappa_{23} \circ \Pi_2 \circ \kappa_{12} \circ \Pi_1,$$

where  $\kappa$  is the change of coordinates defined in Lemma 6.2 and  $\Pi_1, \Pi_2, \Pi_3$  are the transition maps in each chart. Finally, reversing the blow up transformation gives the full transition map  $\pi$  and therefore there exists a trajectory  $\gamma$  in the blow down vector field connecting slow and fast flow. With this analysis at hand we are now able to describe the full dynamics of the Van der Pol system when  $\epsilon > 0$  by analysing the singular limit  $\epsilon \rightarrow 0$ . The full result is visualised in Figure 1.



(a) The flow on the Van der Pol for a small  $\epsilon$ .

(b) The flow on the Van der Pol for a larger  $\epsilon$ .

Figure 6: Flow on the Van der Pol system.

## 7 Canard Points

Considering the Van der Pol System as before:

$$\begin{aligned} x' &= -y + x^2 - \frac{x^3}{3}, \\ y' &= \epsilon(x - 1), \end{aligned} \tag{13}$$

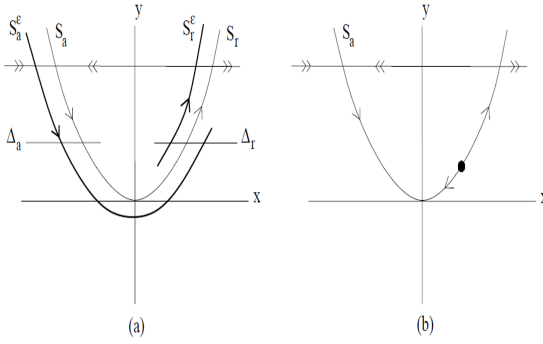


Figure 7: The reduced flow where a)  $\lambda = 0$  and b)  $\lambda > 0$ .

we notice that the equilibrium of the system depends on the two nullclines  $x' = 0$  and  $y' = 0$ . These are in the shape of a cubic function and in the shape of a vertical line at  $x = 1$ . The idea in this section is to replace the nullcline  $x = 1$  by  $x = \lambda$ . This can be seen as shifting the equilibrium of the system along the critical manifold  $S$  by varying the parameter  $\lambda$ . This gives rise to a generalised Van der Pol system:

$$\begin{aligned} x' &= -y + x^2 - \frac{x^3}{3}, \\ y' &= \epsilon(x - \lambda). \end{aligned} \tag{33}$$

In this section, the dynamics in system 36 is analysed. In order to do so, we need the definition of a canard.

**Definition 7.1. Canard**[Kuehn 2015] A trajectory of a fast-slow system is called a canard if it stays within  $O(\epsilon)$  close to the repelling branch  $S^r$  of the slow manifold  $S$ , for some time of  $O(1)$  on the slow time scale  $\tau = \epsilon t$ .

Furthermore, the following definition turns out to be useful as well:

**Definition 7.2. Maximal Canard**[Kuehn 2015] The trajectory passing through the intersection of  $S^a$  and  $S^r$  is called a maximal canard.

The intuition of the canard problem close to a fold point is given in Figure 7.

Equivalently to the analysis of the fold point in Section 5, some nondegeneracy conditions are defined. These are, as before, applied at the fold point  $(0,0)$ . Note that in contrast to the nondegeneracy conditions in (6), the transversality condition  $g(0,0,0) \neq 0$  is not satisfied. Therefore higher order conditions on  $g$  have to be employed, in particular these are nonzero derivatives of  $g$  with respect to  $x$  and  $\lambda$ . The fact that  $g_x(0,0,0) \neq 0$  guarantees the existence of transversal intersection of the two nullclines, which is crucial in order to conclude persistence of the dynamics later on (?). ++  $g_\lambda$  gives nonzero speed condition (why is that a condition?)+++ The nondegeneracy and transversality conditions for the canard case are:

$$f(0,0,0,0) = 0, \quad \frac{\partial}{\partial x} f(0,0,0,0) = 0, \quad g(0,0,0,0) = 0, \tag{34}$$

$$\begin{aligned} \frac{\partial^2}{\partial x^2} f(0,0,0,0) &\neq 0, \quad \frac{\partial}{\partial y} f(0,0,0,0) \neq 0, \\ \frac{\partial}{\partial x} g(0,0,0,0) &\neq 0, \quad \frac{\partial}{\partial \lambda} g(0,0,0,0) \neq 0. \end{aligned} \tag{35}$$

(Krupa & Szmolyan 2001).

Now that these conditions have been defined we can consider, equivalent to the argument in Section 5.6, the extended Van der Pol system,

$$\begin{aligned} x' &= -y + x^2 - \frac{x^3}{3}, \\ y' &= \epsilon(x - \lambda), \\ \epsilon' &= 0, \\ \lambda' &= 0, \end{aligned} \tag{36}$$

where the change in  $\epsilon$  and  $\lambda$  are constant. Now, for the remainder of the section, we apply the method of Krupa & Szmolyan (2001) to the Van der Pol System. The canonical form for the Canard System is:

$$\begin{aligned} x' &= -yh_1(x, y, \epsilon, \lambda) + x^2h_2(x, y, \epsilon, \lambda) + \epsilon h_3(x, y, \lambda, \epsilon) \\ &= -y + x^2 \left(1 - \frac{x}{3}\right), \\ y' &= \epsilon(xh_4(x, y, \epsilon, \lambda) - \lambda h_5(x, y, \epsilon, \lambda) + yh_6(x, y, \lambda, \epsilon)) \\ &= \epsilon(x - \lambda). \end{aligned} \tag{37}$$

It follows that  $h_1 = 1$ ,  $h_2 = 1 - \frac{x}{3}$ ,  $h_3 = 0$ ,  $h_4 = 1$ ,  $h_5 = 1$  and  $h_6 = 0$ . It is possible to find a  $\lambda > 0$ , for which an equilibrium on the repelling branch  $S_r$  exists for the reduced dynamics. The following definition can be made in order to simplify the following computations:

$$\begin{aligned} a_1 &= \frac{\partial}{\partial x} h_3(0, 0, 0, 0) = 0 & a_2 &= \frac{\partial}{\partial x} h_1(0, 0, 0, 0) = 0 & a_3 &= \frac{\partial}{\partial x} h_2(0, 0, 0, 0) = -\frac{1}{3} \\ a_4 &= \frac{\partial}{\partial x} h_4(0, 0, 0, 0) = 0 & a_5 &= h_6(0, 0, 0, 0) = 0. \end{aligned}$$

Furthermore, we can define the quantity:

$$A = -a_2 + 3a_3 - (2a_4 + 2a_5) = -1,$$

which is important in the following analysis, in particular for  $A \neq 0$  (Krupa & Szmolyan 2001). Similar to the procedure in Section 6, sections of the dynamical system can be defined, in order to monitor the in- and outgoing trajectories. In this case we are interested in two sections of the neighbourhood  $U$ , defined as in Section 6, that monitor  $S^a$  and  $S^r$  close to the fold point. Let  $\Delta_a = \{(x, \rho^2), x \in I_a\}$  and  $\Delta_r = \{(x, \rho^2), x \in I_r\}$ , where  $I_a, I_r$  are intervals on the real line and  $\rho$  is sufficiently small. Furthermore, define  $q_a$  to be the point on  $\Delta_a$  that belongs to the attracting branch  $S^a$ , while  $q_r$  is equivalently defined as the point on  $\Delta_r$  that corresponds to  $S^r$ . Finally, we are in the position to define the transition map  $\pi : \Delta^a \rightarrow \Delta^r$ , compare to Section 6.

Following this, Krupa & Szmolyan (2001) discuss the existence of a critical value for  $\lambda$  (denoted  $\lambda_c$ ), where the two branches  $S_r$  and  $S_a$  must connect in a smooth fashion. The transition map  $\pi$  has to map the point  $q_a$  to  $q_r$ , if the branches are connected, and the trajectory passing through the fold point is called the maximal canard, see Definition 7.2. The following theorem describes the technical details involved, and some of the results are derived by the following analysis.

**Theorem 7.3** (Krupa & Szmolyan (2001))

Assume that system (3.1) satisfies the defining non-degeneracy conditions (Equations 34 and 35) of a canard point. Assume that the solution  $x_0(t)$  of the reduced problem connects  $S_a$  to  $S_r$ . Then there exists  $\epsilon_0 > 0$  and a smooth function  $\lambda_c(\sqrt{\epsilon})$  defined on  $[0, \epsilon_0]$  such that for  $\epsilon \in (0, \epsilon_0)$  the following assertions hold:

—  $\pi(q_{a,\epsilon}) = q_{r,\epsilon}$  iff  $\lambda = \lambda_c(\sqrt{\epsilon})$ .

— The function  $\lambda_c$  has the expansion

$$\lambda_c(\sqrt{\epsilon}) = -\epsilon \left( \frac{a_1 + a_5}{2} + \frac{A}{8} \right) + O(\epsilon^{\frac{3}{2}}).$$

— The transition map  $\pi$  is defined only for  $\lambda$  in an interval around  $\lambda_c(\sqrt{\epsilon})$  of width  $O(\exp(-\frac{c}{\epsilon}))$  for some  $c > 0$ .

$$\frac{\partial}{\partial \lambda} (\pi(q_{a,\epsilon}) - q_{r,\epsilon})|_{\lambda=\lambda_c(\sqrt{\epsilon})} > 0$$

Consider Canard cycles and center manifolds / Freddy Dumortier, Robert Roussarie. for more details on canards in Van der Pol . ++++++Kieran, what do you mean here++++

## 7.1 Canard Blow-up

Now similarly to Section 6, we consider a transformations of the coordinate system in order to analyse the dynamics in the neighbourhood of the non-hyperbolic equilibrium induced by the canard point (++++++ is the eq. induced by lambda??++++)+. The transformations are taken from ([Krupa & Szmolyan 2001](#)) and are:

$$x = \bar{r}\bar{x}, \quad y = \bar{r}^2y, \quad \epsilon = \bar{r}^2\bar{\epsilon}, \quad \lambda = \bar{r}\bar{\lambda}. \quad (38)$$

Now that we have established these transformation, the charts  $K_1$  and  $K_2$  can be introduced, but it is not necessary to consider the third chart,  $K_3$ . Since the attracting slow manifold connects to the repelling slow manifold, the flow will ‘bend back’ from  $K_2$  into  $K_1$  instead of leaving the neighbourhood  $U$  in the direction of the fast flow, which was described by  $K_3$  in Section 6. This pheonomenon can be observed in Figure 8, where the trajectory stays close to  $S^r$  after passing the fold point.

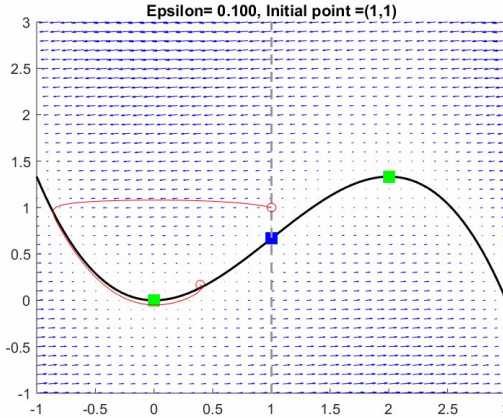


Figure 8: The Van der Pol system for the canard case.

Again, equivalently to the procedure in Section 6, we can define the coordinate transformation for the charts. Note, that in contrast to the generic Blow-Up in Section 6, the coordinate system is now in  $\mathbf{R}^4$ , and not in  $\mathbf{R}^3$ . In chart  $K_1$ ,  $y_1 = 1$ , while in  $K_2$ ,  $\epsilon_1 = 1$  and then:

$$x = r_1 x_1, \quad y = r_1^2, \quad \epsilon = r_1^2 \epsilon_1, \quad \lambda = r_1 \lambda_1 \quad (39a)$$

$$x = r_2 x_2, \quad y = r_2^2 y_2, \quad \epsilon = r_2^2, \quad \lambda = r_2 \lambda_2. \quad (39b)$$

Furthermore, we can define the coordinate change between the two charts as follows:

**Lemma 7.4**

Let  $\kappa_{12}$  denote the change of coordinates from  $K_1$  to  $K_2$ . Then  $\kappa_{12}$  is given by

$$x_2 = x_1 \epsilon_1^{-1/2}, \quad y_2 = \epsilon_1^{-1}, \quad r_2 = r_1 \epsilon_1^{1/2}, \quad \lambda_2 = \epsilon_1^{-1/2} \lambda_1,$$

for  $\epsilon_1 > 0$ . Similarly  $\kappa_{21} = \kappa_{12}^{-1}$  is given by

$$x_1 = x_2 \epsilon_1^{-1/2}, \quad r_1 = r_2 \epsilon_1^{1/2}, \quad \epsilon_1 = y_2^{-1}, \quad \lambda_1 = \lambda_2 y_2^{-1/2},$$

for  $y_2 > 0$ .

We are now in the position to begin with the analysis in the charts, and will first consider chart  $K_2$ , since, as in Section 6,  $K_2$  holds the most information.

### 7.1.1 Dynamics in $K_2$

||||| HEAD We start by noting that we are considering our invariant plane at  $r_2 = 0$  which will significantly simplify our system for  $K_2$ . Further we should note that we are taking a transformation in time,  $\frac{dr}{dt_2} = \frac{dt}{dt_2} \frac{dr}{dt} = \frac{1}{r_2} \frac{dr_2}{dt}$ , as well as in our coordinates. Then if we substitute our time transformation and Equation 39b into our system of Equations 36 we find,

$$\begin{aligned} r_2^2 x'_2 - r_2 x_2 r'_2 &= -r_2^2 y_2 h_1 + r_2^2 x_2^2 h_2, \\ \implies x'_2 &= -y_2 + x_2^2 - r_2 G_2(x_2, y_2), \end{aligned} \quad (40a)$$

$$\begin{aligned} r_2^3 y'_2 - 3r_2^2 y_2 r'_2 &= r_2^2 (r_2 x_2 h_4 - r_2 \lambda_2 h_5), \\ \implies y'_2 &= x_2 - \lambda_2 + r_2 G_2(x_2, y_2), \end{aligned} \quad (40b)$$

where we note that  $h_j = h_j(x, y, \epsilon, \lambda)$  for  $j = 1, 2, 3, 4, 5$ . We should also recall that  $r'_2 = \lambda'_2 = 0$ . Notice that we have included an additional term in Equation 40b - we define  $G_2(x_2, y_2)$  in the following way,  $G(x_2, y_2) = (G_1(x_2, y_2), G_2(x_2, y_2))^T = (-\frac{x_2^3}{3}, 0)^T$ . The reason we also define this vector is to aide in the Melnikov computations which we will see later. Krupa & Szmolyan (2001) discusses that for this chart we have an interesting result. They note that at  $r_2 = \lambda_2 = 0$  our system is integrable which allows us to define a constant of motion  $H(x_2, y_2) = \frac{1}{2} \exp(-2y_2) (y_2 - x_2^2 + \frac{1}{2})$  which we can easily verify (Krupa & Szmolyan 2001) using the following equations, ===== The transformations 39b, as well as a transformation in time,  $\frac{dr}{dt_2} = \frac{dt}{dt_2} \frac{dr}{dt} = \frac{1}{r_2} \frac{dr_2}{dt}$ , is applied to system (37), which results in

$$\begin{aligned} r_2^2 x'_2 - r_2 x_2 r'_2 &= -r_2^2 y_2 + r_2^2 x_2^2 \left(1 - \frac{x}{2}\right), \\ r_2^3 y'_2 - 3r_2^2 y_2 r'_2 &= r_2^2 (r_2 x_2 - r_2 \lambda_2). \end{aligned}$$

Since  $r' = 0, \lambda' = 0$ , from the extended system, the resulting system is:

$$x'_2 = -y_2 + x_2^2 - r_2 G_1(x_2, y_2) = -y_2 + x_2^2 - r_2 \left( -\frac{x_2^3}{3} \right), \quad (41)$$

$$y'_2 = x_2 - \lambda_2 + r_2 G_2(x_2, y_2) = x_2 - \lambda_2. \quad (42)$$

Then, in vector form  $G(x_2, y_2)$  is defined in the following way,  $G(x_2, y_2) = (G_1(x_2, y_2), G_2(x_2, y_2))^T = (-\frac{x_2^3}{3}, 0)^T$ . This quantity will become relevant at a later point, when the Melnikov computation is considered. [Krupa & Szmolyan \(2001\)](#) discusses that for  $r_2 = \lambda_2 = 0$  the system is integrable. The system (42) reduces to:

$$\begin{aligned} x'_2 &= -y_2 + x_2^2 \\ y'_2 &= x_2. \end{aligned}$$

Since this system is integrable, a constant of motion  $H$  can be found in the following way. Firstly, expand each of the equations by the factor  $e^{2y_2}e^{-2x_2} = 1$ , and define parts of the equations as partial derivatives of  $H$ , which results in:

$$\begin{aligned} x'_2 &= e^{2y_2}e^{-2y_2}(-y_2 + x_2^2) = e^{2y_2} \frac{\partial H}{\partial y_2}(x_2, y_2) \\ y'_2 &= -e^{2y_2}e^{-2y_2}(-x_2) = -e^{2y_2} \frac{\partial H}{\partial x_2}(x_2, y_2). \end{aligned}$$

Then, the partial derivatives in  $H$  are integrated as follows:

$$\begin{aligned} \frac{\partial H}{\partial x_2}(x_2, y_2) &= -e^{-2y_2}x_2 \\ \Rightarrow H(x_2, y_2) &= \int -e^{-2y_2}x_2 dx \\ \Rightarrow H(x_2, y_2) &= -\frac{1}{2}x_2^2e^{-2y_2} + C(y), \end{aligned}$$

where  $C(y)$  is the constant of integration, which could depend on  $y$ . Then, by taking the derivative with respect to  $y$  and setting it equal to the expression  $\frac{\partial H}{\partial y_2}(x_2, y_2) = e^{-2y_2}(-y_2 + x_2^2)$ , defined above, we can find the value for  $C(y)$  as follows:

$$\begin{aligned} \frac{\partial H}{\partial y_2}(x_2, y_2) &= x_2^2e^{-2y_2} + C'(y) \\ &= e^{-2y_2}(-y_2 + x_2^2) \\ \Rightarrow C'(y) &= -y_2e^{-2y_2} \end{aligned}$$

In a last step, we can integrate  $C'(y)$  in order to find an explicit expression for  $H$ :

$$C(y) = \int -y_2e^{-2y_2} dy = \frac{1}{2}y_2e^{-2y_2} + \frac{1}{2}e^{-2y_2} + c,$$

using integration by parts, and where  $c$  is the constant of integration. Then, the final expression for the constant of motion is:

$$\begin{aligned} H(x_2, y_2) &= -\frac{1}{2}x_2^2e^{-2y_2} + \frac{1}{2}y_2e^{-2y_2} + \frac{1}{2}e^{-2y_2} + c \\ &= \frac{1}{2}e^{-2y_2} \left( y_2 - x_2^2 + \frac{1}{2} \right) + c. \end{aligned}$$

Note that without loss of generality  $c = 0$ , because we are interested in the level curves of  $H$ ,  $H = h$ , and therefore an additional constant just represents a shift of the level curve. Then the expression for  $H$  is comparable with the result in [? . , iiii.lli fc965573a42105f0cc649fd2b72dfcb929fc097a](#)

$$x'_2 = e^{2y_2} \frac{\partial H}{\partial y_2}(x_2, y_2), \quad (43a)$$

$$y'_2 = -e^{2y_2} \frac{\partial H}{\partial x_2}(x_2, y_2). \quad (43b)$$

Further to this we can see, when we consider our reduced system, that we have an equilibrium at the origin, implying that  $H(x_2, y_2) = h$ . considering the reduced system (Equation 42) we find from  $H(x_2, y_2) = 0$  that,

$$x'_2 = \frac{1}{2} \implies x_2 = \frac{t_2}{2} + A, \quad (44a)$$

$$y'_2 = \frac{t_2}{2} \implies y_2 = \frac{t_2^2}{4} - \frac{1}{2}, \quad (44b)$$

where we have directly integrated Equation 44a with respect to our time ( $t_2$ ). However, we can note that we are able to choose  $A = 0$  as we are considering an autonomous (time-invariant) system. Then for Equation 44b we are able to rearrange constant of motion at zero to give,  $y_2 = x_2^2 - \frac{1}{2}$ . Clearly from this analysis we are then able to define our trajectories in terms of  $\gamma_{c,2}$ ,

$$\gamma_{c,2}(t_2) = (x_{c,2}(t_2), y_{c,2}(t_2)) = \left( \frac{t_2}{2}, \frac{t_2^2}{4} - \frac{1}{2} \right). \quad (45)$$

Now that we have established that we must have a flow on our second chart, then there must also exist transition maps. Therefore this now enables us to consider the first chart in the following section.

### 7.1.2 Dynamics in $K_1$

For  $K_1$  we follow a similar approach to the above. We will use the transformations,

$$x = r_1 x_1, \quad y = r_1^2, \quad \epsilon = r_1^2 \epsilon_1, \quad \lambda = r_1 \lambda_1, \quad (39a)$$

to find the relevant pathways of our flows. Now if we first consider the  $r_1$  component,

$$2r_1^2 r'_1 = r_1^2 \epsilon (r_1 x_1 - r_1 \lambda_1), \quad (46)$$

where we can call  $F = F(x, y, \epsilon, \lambda) = x_1 - \lambda_1 + O(r_1(r_1 + \lambda_1))$ . Now we will see the motivation with starting with  $y = r_1$  when we transform our other coordinates. Now if we consider  $x = r_1 x_1$ ,

$$x'_1 = -1 + x_1^2 - \frac{x_1 r'_1}{r_1},$$

where we can use Equation 46 to simplify this further - Equation 47.

$$x'_1 = -1 + x_1^2 - \frac{x_1}{r_1} \left( \frac{r_1 \epsilon_1 F}{2} \right) \quad (47)$$

We now consider our  $\epsilon = \epsilon_1 r_1^2$  and noting  $\epsilon' = 0$ . Then we have,  $r_1^3 \epsilon' = -2r_1^2 \epsilon_1 r_1'$ , where we can use Equation 46 to simplify to,

$$\epsilon' = -\epsilon_1^2 F. \quad (48)$$

Our last transformation is for our new coordinate  $\lambda = r_1 \lambda$ , noting that  $\lambda' = 0$ . Similarly to the above we find  $r_1^2 \lambda'_1 + r_1 \lambda_1 r'_1 = 0$  then,

$$\lambda'_1 = -\frac{\lambda_1 \epsilon_1 F}{2}, \quad (49)$$

which is a trivial rearrangement as seen in Equation 48. Now if we combine the above we find that our transformed system is of the following form,

$$r'_1 = \frac{\epsilon}{2}(r_1 x_1 - r_1 \lambda_1), \quad (50a)$$

$$x'_1 = -1 + x_1^2 - \frac{x_1 \epsilon_1 F}{2}, \quad (50b)$$

$$\epsilon' = -\epsilon_1^2 F, \quad (50c)$$

$$\lambda'_1 = -\frac{\lambda_1 \epsilon_1 F}{2}. \quad (50d)$$

From this system we are now able to make some deductions. We first can observe that the hyperplanes are along the  $r_1 = \epsilon_1 = \lambda_1 = 0$  with an invariant line at  $l_1 = \{(x_1, 0, 0, 0) : x_1 \in \mathbb{R}\}$  (Krupa & Szmolyan 2001). As Krupa & Szmolyan (2001) discusses the equilibria present at the end of both of our branches - Figure 7 - which are found at  $p_a = (-1, 0, 0, 0)$  and  $p_r = (1, 0, 0, 0)$  (Krupa & Szmolyan 2001). Now we can go one step further, we can consider Equation 50 and find the eigenvalues of the system for the invariant planes. We find that,

$$J - \sigma I = \begin{bmatrix} 2x - \sigma & 0 & 0 & 0 \\ 0 & -\sigma & 0 & 0 \\ 0 & 0 & -\sigma & 0 \\ 0 & 0 & 0 & -\sigma \end{bmatrix}, \quad (51)$$

which clearly has three zero eigenvalues and one non-zero eigenvalue  $\lambda = \pm 2$ . Which further emphasises that our equilibrium point is non-hyperbolic. As a result we intuitively expect that something interesting occurs at this point. In the section following we will be considering what effect these mappings and eigenvalues will have on our system.

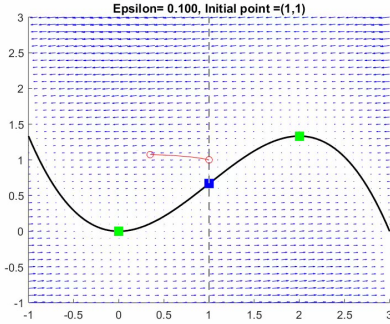
## 7.2 Effect of the Canard Point

Now that we have shown that there must exist a flow around our fold point we should now consider the global effect of the canard point. We can see by considering the system of Equations 50 that our equilibria are at  $(x, y) = (\lambda, \lambda^2[\frac{1-\lambda}{3}])$  and find the eigenvalues from the matrix,

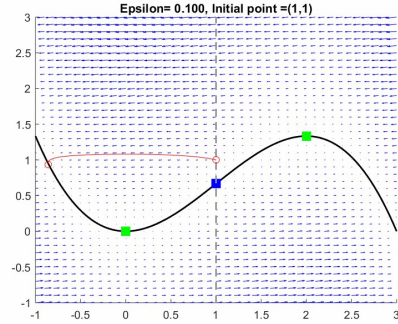
$$A - \sigma I = \begin{bmatrix} 2x - x^2 - \sigma & -1 & 0 & 0 \\ \epsilon & -\sigma & x - \lambda & -\epsilon \\ 0 & 0 & -\sigma & 0 \\ 0 & 0 & 0 & -\sigma \end{bmatrix} = \sigma^2(\sigma^2 + \sigma(x^2 - 2x) + \epsilon). \quad (52)$$

From this we are about to find the eigenvalues of the system,  $\sigma = 0$  and  $\sigma = \frac{2x - x^2 \pm \sqrt{(x^2 - 2x)^2 - 4\epsilon}}{2}$ . Then we consider the values at our equilibrium,  $x = \lambda$ , to find that we have a Hopf Bifurcation when  $4\epsilon > (x^2 - 2x)^2$  or when  $\lambda = 2$  or  $0$ . This then leads to the following trajectories within the flow - Figure 9.

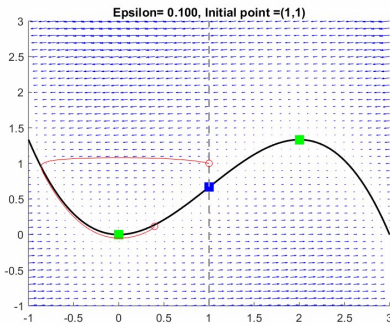
From Figure 9 we can see the progression of our flow over the system. From Figure 9a we see that the flow starts at an initial condition of  $(x, y) = (1, 1)$  and travels along the fast flow towards the attracting branch. Then from Figure 9b the flow has hit the attracting branch, where it then follows along the slow flow towards the



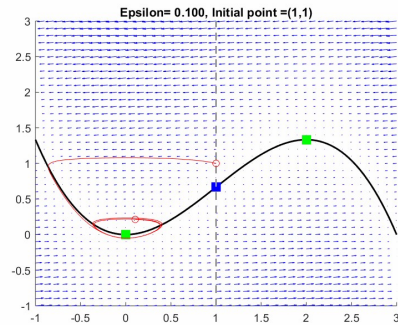
(a) The initial flow within the system.



(b) The flow as it hits the slow manifold.



(c) The flow as it intersects with the fold point.



(d) The Hopf bifurcation due to the canard point.

Figure 9: The trajectories associated with the canards case of the Van der Pol system.

fold point at  $(x, y) = (0, 0)$ , which is described by Figure 9c. Then from Figures 9c and 9d we can observe the Hopf bifurcation. This is because we make note that the canard point is present at  $-\lambda$ , which in essence pushes the flow up the repelling branch (see Figure 7) until the flow is sufficiently far from the fold point where it will then repel towards the attracting branch, starting the oscillation - Figure 9d. Moreover, it is worth noting that our Hopf bifurcation only exists when we are in an arbitrarily small region,  $O(\epsilon)$  [Eckhaus \(1970\)](#) - this idea is further discussed in Section 7.2.1.

### 7.2.1 Singular Hopf Bifurcation

Furthermore, in the Van der Pol we are able to find a singular Hopf Bifurcation when  $\lambda = 1$ . Then to model this behaviour we need to consider a small perturbation along the slow flow where we will have, from Equation 36,

$$\dot{y} = \lambda - x + \bar{\nu}y, \quad (53)$$

where  $\nu$  is of order  $O(\epsilon)$ , thus small. We can immediately see that when  $\bar{\nu} = 0$  that we have our original flow at our equilibrium but we are now able to perturb our flow over a small domain, which are described in Figures ???. We can also see how our system behaves when our  $\nu$  is of larger order than  $O(\epsilon)$ ,

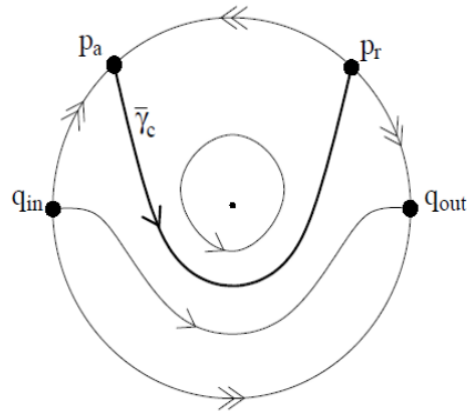


Figure 10: The flow within our canard system ([Krupa & Szmolyan 2001](#)).

where it is clear that our Hopf bifurcation is the periodic solution in the centre of Figure 10 but we can see that below our special flow  $\bar{\gamma}_c$  (for the flow outside of the domain  $O(\epsilon)$ ), our solution traverses through our equilibrium into our fast flow as we would expect in our original system.

### 7.2.2 Separation of the Manifolds

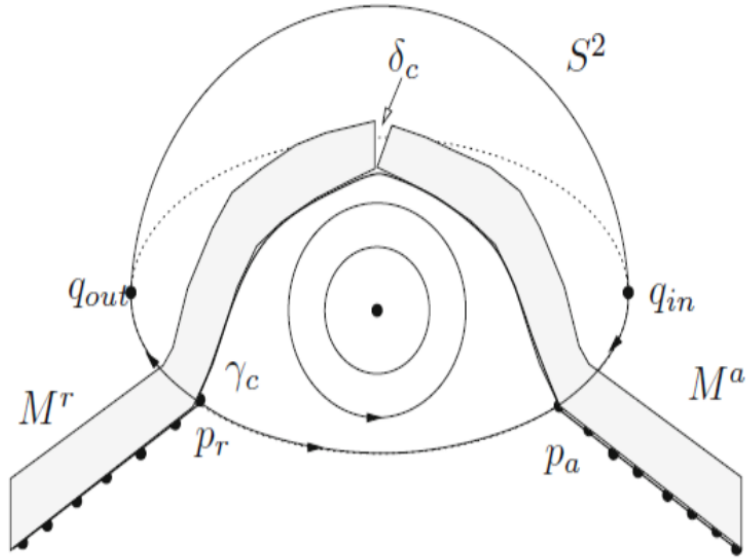


Figure 11: Separation of  $M_a$  and  $M_r$  ([Kuehn 2015](#)).

Continuing on from the singular Hopf bifurcation we might find that the canard point forces our branches to split. In other words we are looking for when the attracting and repelling branches are no longer connected, as shown in Figure 11. To do this we would use Melnikov Computations to show that our manifolds split - see *Extending Geometric Singular Perturbation Theory to Nonhyperbolic Points - Fold and Canard Points in Two Dimensions* ([Krupa & Szmolyan 2001](#)) for direct use. To discover whether we have a splitting between our branches we need

to consider our  $y$  coordinates with respect to our second chart such that  $y_{a,2}(0) - y_{r,2}(0)$  is a distance function which can be written as  $D_c(r_2, \lambda_2) = H(0, y_{a,2}(0)) - H(0, y_{r,2}(0))$  as we note that  $\frac{\partial}{\partial y_2} H(0, y_2) \neq 0$  ([Krupa & Szmolyan 2001](#)). From here we can use the following proposition,

**Proposition 7.5** ([Krupa & Szmolyan 2001](#))

For a small enough  $\rho$  and  $\mu$  the distance function has the expansion

$$D_c(r_2, \lambda_2) = d_{r_2} r_2 + d_{\lambda_2} \lambda_2 + O(2),$$

where we have defined,

$$d_{r_2} = \int_{-\infty}^{\infty} \text{grad}H(\gamma_{c,2}(t)) \cdot G(\gamma_{c,2}(t)) dt, \quad (54a)$$

$$d_{\lambda_2} = \int_{-\infty}^{\infty} \text{grad}H(\gamma_{c,2}(t)) \cdot (0, -1)^T, \quad (54b)$$

and our matrix  $G(\gamma_{c,2}(t))$  in Section 7.1.2 with  $\gamma_{c,2}$  as our critical trajectory.

Then, following the proof provided by [Krupa & Szmolyan \(2001\)](#), we find that we will have a split occurring between our branches if the canard falls outside of our domain of order  $O(e^{-\frac{c}{\epsilon}})$  such that  $D_c(r_2, \lambda_2) \neq 0$ . As a result of we see a flow similar to Figure 11 whereby we find that our flow could either jump off under the fast flow - see Figure 6 - or we might find that the flow could be trapped in the canard region and then be repelled back to the attracting manifold, as we see with our connected system - Figure 9.

Good to have a figure if possible

## 8 Folded Singularities in a Three Dimensional System

Now that we have considered the two dimensional case for a folded singularity we can extend it to a third dimension in our system. This can be done by considering a system of one fast and two slow variables such that,

$$\begin{cases} \epsilon x' = f(x, y, z, y, \epsilon), \\ y' = g_1(x, y, z, y, \epsilon), \\ z' = g_2(x, y, z, y, \epsilon), \end{cases} \quad (55)$$

which we can see is an extension of our original form - Equation 2 ([Desroches et al. 2012](#)). Furthermore, [Desroches et al. \(2012\)](#) also discusses that the addition of an extra slow variable causes issues with respect to the existence of a canard solution. This is because our existence ranges increases from  $O(\epsilon)$  to  $O(1)$ , noting that  $\epsilon \ll 1$  ([Desroches et al. 2012](#)). Then for this system we are able to make similar assumptions to the previous case, Section 4, but it is obvious we now must have more than one fold point. We can see that this is the case in Figure 12,

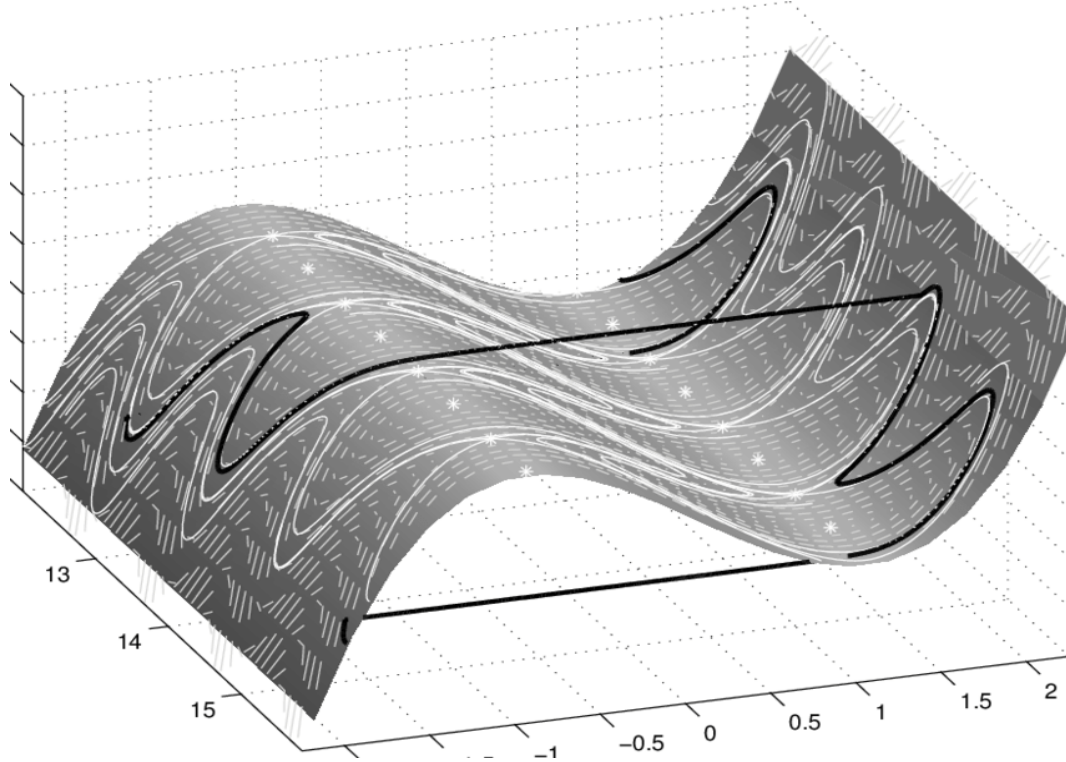


Figure 12: Three dimensional Van der Pol ([Festschrift et al. 2001](#)).

as our fold point now can take multiple locations within our system, denoted by ‘\*’. From here we are able to define some non-degeneracy conditions, much like we did in Section 3,

$$\begin{aligned}
 f(p_*, \lambda, 0) &= 0, \\
 \frac{\partial}{\partial x} f(p_*, \lambda, 0) &= 0, \\
 \frac{\partial^2}{\partial x^2} f(p_*, \lambda, 0) &\neq 0, \\
 D_{(y,z)} f(p_*, \lambda, 0) \text{ has full rank one,}
 \end{aligned} \tag{56}$$

where we denote  $p_* = (x_*, y_*, z_*) \in F$  as our fold points and  $D_{(y,z)} = (\frac{\partial f}{\partial y}, \frac{\partial f}{\partial z})$  are **linearly independent of one another** ([Desroches et al. 2012](#)). In addition to this we can see from Figure 12 that we have some interesting flows within our system. These flows do not follow the standard pattern as we saw in Figure 1, instead the slow flow switches its orientation when the flow hits the fold point and continue to flow in that direction, as a desingularised flow - these are called isolated singularities ([Desroches et al. 2012](#)). As a result we are able to write these flows in the following manner, using Equations 55, 56 and noting that  $\frac{dx}{dt} = 0 = \frac{\partial f}{\partial x}$ ,

$$-\frac{\partial f}{\partial x} x' = y' \frac{\partial f}{\partial y} + z' \frac{\partial f}{\partial z}, \tag{57}$$

where we can note that  $y' = g_1$  and  $z' = g_2$ . We then make a scaling in time such that  $t = -\frac{\partial f}{\partial x}$  wto give the system in the desired form,

$$\begin{cases} \dot{x} = g_1 \frac{\partial f}{\partial y} + g_2 \frac{\partial f}{\partial z}, \\ \dot{y} = -g_1 \frac{\partial f}{\partial x}, \\ \dot{z} = -g_2 \frac{\partial f}{\partial x}. \end{cases} \quad (58)$$

From here we can then define a folded singularity if  $g_1(p_*, \lambda, 0) \frac{\partial}{\partial y} f(p_*, \lambda, 0) + g_2(p_*, \lambda, 0) \frac{\partial}{\partial z} f(p_*, \lambda, 0) = 0$ , for our flow on branches ( $S$ ) (Desroches et al. 2012). Next we need to consider the stability of our fold points. We do this by constructing the Jacobian of our system,

$$J = \begin{bmatrix} \frac{\partial \dot{x}}{\partial x} & \frac{\partial \dot{x}}{\partial y} & \frac{\partial \dot{x}}{\partial z} \\ \frac{\partial \dot{y}}{\partial x} & \frac{\partial \dot{y}}{\partial y} & \frac{\partial \dot{y}}{\partial z} \\ \frac{\partial \dot{z}}{\partial x} & \frac{\partial \dot{z}}{\partial y} & \frac{\partial \dot{z}}{\partial z} \end{bmatrix}, \quad (59)$$

which we can easily find the eigenvalues, by taking the determinant. The result of this analysis gives that we have three eigenvalues,  $\sigma_i$  for  $i = 1, 2, 3$  (Desroches et al. 2012). Without loss of generality we can choose  $\sigma_3 = 0$  because we know that at least one of our eigenvalues must be zero to account for our fold point in our system - see the Poincaré diagram for further intuition. Then we know from standard stability theory that, at our folded singularity we will have three types of phase portrait in the form of,

$$\begin{cases} Saddle \ \sigma_1 \sigma_2 < 0 : \sigma_i \in \Re, \\ Node \ \sigma_1 \sigma_2 > 0 : \sigma_i \in \Re, \\ Focus \ \sigma_1 \sigma_2 > 0 : \Im(\sigma_i) \neq 0, \end{cases} \quad (60)$$

where we can note that only our focus will have imaginary parts (Desroches et al. 2012). Desroches et al. (2012) illustrates this in the following Figure,

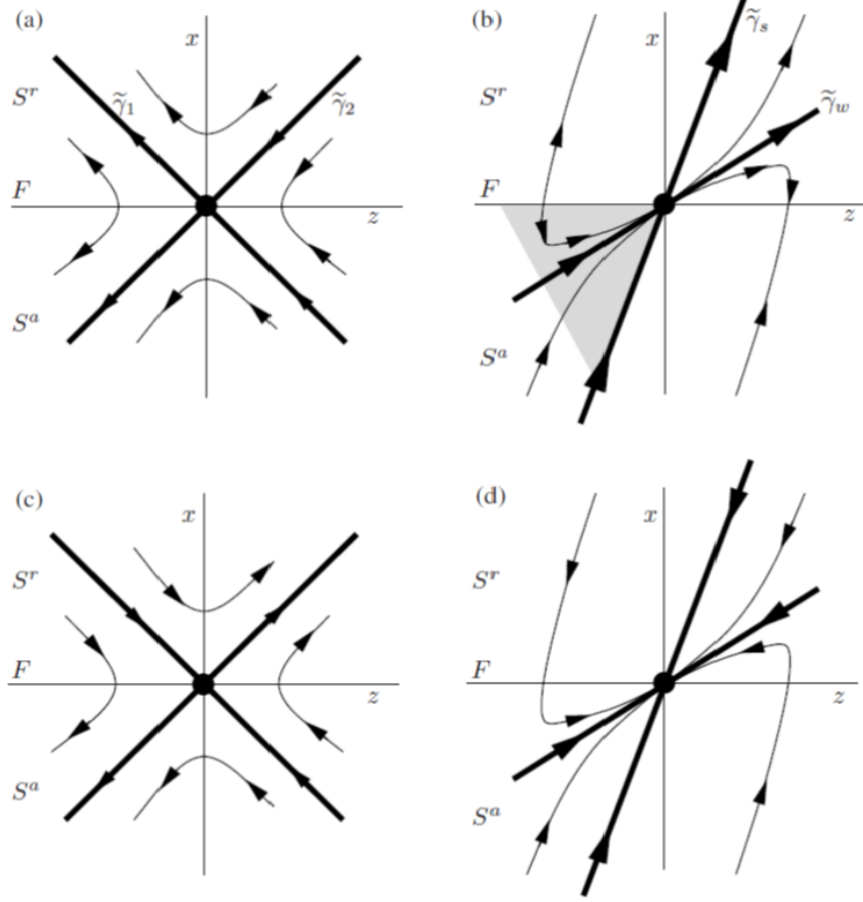


Figure 13: Phase portraits of our three dimensional system where a) is a folded saddle, b) folded node, c) and d) are desingularised flows ([Desroches et al. 2012](#)).

where we can see the effect of the varying eigenvalues above. A question which is prudent to consider is, why has not ([Desroches et al. 2012](#)) illustrated the singular canard case for a folded focus. This is easily answered as we know that a singular canard is only present if the node or saddle connect our two connecting branches ( $S^r$  and  $S^a$ ). The idea that our branches are connected allows us to note that our flow is able to pass through from an attracting to a repelling manifold, which is described by Figure 13 ([Szmolyan & Wechselberger 2001](#)). However, we find that for the focus we are unable to construct branches which connect, preventing the flow from traversing through the fold point. This idea is easily seen as we are able to note, from the imaginary eigenvalues, that there is a spiral present - Figure 14.

Figure 14: The branches of a spiral

It is easily seen, from Figure 14, that it is not possible to construct such a system that allows the flow to traverse this point. We can add further intuition to this example by considering the notion of a source (or sink), which is seen in dynamical systems and fluid mechanics. From a sink (attracting manifold) we know that our flow will always be travelling towards the singularity regardless of its starting location as described by Figure 14 meaning that is impossible to construct a repelling manifold which can connect with this singularity at the fold point - for further information see Figure ?? in Appendix ??, where we can see that we are unable to produce a system which has a singular

**Theorem 8.1** (Canards in  $\mathbb{R}^3$  (Desroches et al. 2012))

For slow-fast systems (Equation 55) with  $\epsilon > 0$  sufficiently small the following holds:

- There are no maximal canards generated by a folded focus. For a folded saddle the two singular canards  $\gamma_{1,2}$  perturb to maximal canards  $\gamma_{1,2}$ .
- For a folded node let  $\mu = \frac{\sigma_w}{\sigma_s} < 1$ . the singular canard  $\bar{\gamma}_s$  (“the strong canard”) always perturbs to a maximal canard  $\gamma_s$ . If  $\mu^{-1} \notin \mathbb{N}$ , then the singular canard  $\bar{\gamma}_w$  (“weak canard”) also perturbs to a maximal canard. We call  $\gamma_s$  and  $\gamma_w$  primary canards.
- For a folded node suppose  $k > 0$  is an integer such that  $2k+1 < \mu^{-1} < 2k+3$  and  $\mu^{-1} \neq 2(k+1)$ . Then, in addition to  $\gamma_{s,w}$  there are  $k$  other maximal canards, which we call secondary canard.
- The primary weak canard of a node undergoes a transcritical bifurcation for odd  $\mu^{-1} \in \mathbb{N}$  and a pitchfork bifurcation for even  $\mu^{-1} \in \mathbb{N}$

From Theorem 8.1 we have now defined the existence of a strong and weak eigenvalue such that  $|\sigma_1| > |\sigma_2| \iff |\sigma_s| > |\sigma_w|$ . From this theorem we are then able to carry out explicit investigations, as we will see in Section **Not done yet** noting that a focus is a circle or spiral etc.

## 9 MMO

### 9.1 Oscillations

In this section we consider Mixed Mode Oscillations (MMOs) in fast-slow systems.++Motivation for studying these+++ ++++ add that we consider the work from the Desroches et al. (2012) paper unless indicated otherwise

**Definition 9.1.** Mixed Mode Oscillations[?][Desroches et al. 2012] A mixed mode oscillation is an orbit  $\gamma$ , which traces out small amplitude oscillations (SAOs) as well as large amplitude oscillations (LAOs). The SAOs and LAOs are clearly separated in the time series and their reoccurrence can be periodic. The signature of an MMO is expressed as  $L_1^{s_1} L_2^{s_2} \dots$ , indicating that  $L$  number of LAOs are followed by  $s$  SAOs.

The cases of MMOs considered here are MMOs associated with folded nodes as well as folded saddle-nodes of type 2, that are associated to singular hopf bifurcations. +++++++needs better intro.++++++

### 9.2 Folded Nodes

In this section the occurrence of different SAOs due to a folded node of the reduced system is discussed and conditions for a global return mechanism, which gives rise to MMOs, are presented. The folded node singularity

is an equilibrium of the reduced system. Note that it is only defined on  $S$ , the critical manifold and therefore only for the slow flow. There is no global equilibrium, which will become apparent in this section. The normal form considered for analysing the folded node singularity is in terms of the space variables  $(u, v, w)$ , and given by:

$$\epsilon \dot{u} = v - u^2$$

$$\dot{v} = w - u$$

$$\dot{w} = -\nu$$

Then the system can be transformed using the following coordinate and time transformation:

$$u = \frac{x}{(1+\mu)^{1/2}}, \quad v = \frac{y}{(1+\mu)}, \quad w = -\frac{z}{(1+\mu)^{3/2}} \quad (61)$$

$$\tau = \frac{\tau_1}{\sqrt{1+\mu}}, \quad (62)$$

where  $\tau_1$  is the original time variable and  $\tau$  is the transformed time variable. Then  $\frac{d\tau}{d\tau_1} = \frac{1}{\sqrt{1+\mu}}$ , and the system becomes:

$$\epsilon \dot{x} = y - x^2 \quad (63)$$

$$\dot{y} = -z - (\mu + 1)x \quad (64)$$

$$\dot{z} = \nu(1+\mu)^2 \quad (65)$$

where  $\mu$  is the eigenvalue ratio from before. This is nearly in the form presented in Desroches et al. (2012), however, the  $z$  equation there is written purely in terms of  $\mu$  as  $\dot{z} = \frac{1}{2}\mu$ . Equating these two representations yields a relationship between  $\mu$  and  $\nu$ :

$$\begin{aligned} \nu(1+\mu)^2 &= \frac{1}{2}\mu \\ \Rightarrow \nu &= \frac{\mu}{2(1+\mu)^2}, \end{aligned}$$

and this is equivalent to

$$\mu = \frac{-1 + \sqrt{1 - 8\nu}}{-1 - \sqrt{1 - 8\nu}},$$

since  $0 < \mu < 1$  and  $\mu \in \mathbf{R}$ . (+++ unsure about reasoning+++)

Note here that the reason that no global equilibrium exists is because 61 can only have an equilibrium if  $\dot{w} = 0$ . This would imply that  $\nu = 0$ , however, as the previous calculations have shown,  $\nu$  is dependent on the eigenvalue ratio  $\mu$ . Since  $\mu \neq 0$  for the folded node, as will be demonstrated below,  $\nu$  cannot be zero. It is now of interest to verify the location of the folded singularity at the origin, and therefore derive the reduced system as well as the eigenvalues for the reduced problem. Consider equation (63) and define  $\dot{x} := f$  as before. The reduced problem, as  $\epsilon \rightarrow 0$  becomes  $f = y - x^2 = 0$ , and therefore the critical manifold is defined as  $S := \{(x, y, z) : y = x^2\}$ , which is an S shaped two dimensional plane. Now that  $f$  is defined explicitly, we can check the nondegeneracy

conditions for a folded singularity, as presented in (56) and get the following results:

$$\begin{aligned} f(x, y, z, \mu, \epsilon) &= 0 \\ \Rightarrow y &= x^2 \end{aligned}$$

$$\begin{aligned} \frac{\partial f}{\partial x}(x, y, z, \mu, \epsilon) &= 2x = 0 \\ \Rightarrow x &= 0 \Rightarrow y = 0 \\ \frac{\partial^2 f}{\partial x^2}(x, y, z, \mu, \epsilon) &= 2 \neq 0 \\ D_{(y,z)}f &= (1, 0) \text{ full rank one.} \end{aligned}$$

This shows that there exists a fold line  $L := (0, 0, z)$  on the slow manifold  $S$ . In order to determine at which value of  $z$  the folded node singularity is located, we have to consider the reduced system of (63), where we replace  $\nu(1 + \mu)^2$  with  $\frac{1}{2}\mu$  for convenience. The aim is to find an equilibrium of the reduced problem, since we know from the theory discussed that the folded singularity is an equilibrium of the slow flow. The reduced problem is:

$$0 = y - x^2 := f \quad (66)$$

$$\dot{y} = -z - (\mu + 1)x \quad (67)$$

$$\dot{z} = \frac{1}{2}\mu \quad (68)$$

Therefore, the slow flow is derived, analogous to Section (I+++ i guess VDP but also after that++). First, the equation  $f = 0$  is considered and it is noted that we can take the derivative with respect to the time variable to get

$$\dot{y} = 2x\dot{x}, \quad (69)$$

and this can be rearranged to give an expression for the dynamics in  $x$  on the slow manifold:

$$\dot{x} = \frac{\dot{y}}{2x},$$

which is singular for  $x = 0$ , which coincides with the fold line. This expression can be desingularised by rescaling time in the whole reduced system by a factor of  $2x$ . This results in

$$\begin{aligned} \dot{x} &= -(\mu + 1)x - z \\ \dot{y} &= -2x(\mu + 1) - 2xz \\ \dot{z} &= x\mu, \end{aligned} \quad (70)$$

however, it can be noted that the equation for  $y$  can be omitted, since the change in  $y$  is directly related to the change in  $x$  by a factor of  $2x$  as stated in equation (69)(+++mention CMT?++). Therefore, the reduced dynamics can be sufficiently described by

$$\begin{aligned} \dot{x} &= -(\mu + 1)x - z \\ \dot{z} &= x\mu. \end{aligned} \quad (71)$$

Now, following the theory for folded singularities, the folded node has to satisfy the condition (+++add name of the condition and generalized statement of it++++)

$$\begin{aligned} -(\mu + 1)x - z &= 0|_{(0,0,z)} \\ \Rightarrow z &= 0, \end{aligned}$$

which leads to the conclusion that the folded singularity, defined on the slow manifold for  $\epsilon \rightarrow 0$  and located on the fold line  $L = (0, 0, z)$ , is given by  $(0, 0, 0)$ , as expected. The next step of the analysis is to verify that the folded singularity at the origin is indeed a folded node. As discussed in Section 8, the classification of the singularities is determined by the eigenvalues of the reduced system. Therefore, the next step is calculating these eigenvalues. The Jacobian of the reduced system (71) is

$$J = \begin{bmatrix} -(\mu + 1) & -1 \\ \mu & 0 \end{bmatrix}, \quad (72)$$

and therefore the characteristic equation yields

$$\begin{aligned} \sigma^2 + (\mu + 1)\sigma + \mu &= 0 \\ \Rightarrow \sigma_1 &= -1 \quad \text{and} \quad \sigma_2 = -\mu. \end{aligned}$$

Since  $\mu$  is the eigenvalue ratio and satisfies  $0 < \mu < 1$ , we can conclude that

$$\sigma_1\sigma_2 = (-1)(-\mu) = \mu > 0,$$

and therefore, by the conditions presented in Section 8, this shows that the folded singularity is in fact a folded node. Note that if we had tried to find the eigenvalues for the full three dimensional reduced system (70) instead, an additional eigenvalue  $\sigma_3 = 0$  would have occurred. This is the eigenvalue that corresponds to the loss of hyperbolicity at the folded node, which is expected for singular points.

In order to analyse the folded node, the system (61) is transformed using the blow up transformation  $u = \epsilon^{1/2}\bar{x}$ ,  $v = \epsilon\bar{y}$ ,  $w = \epsilon^{1/2}\bar{z}$  and  $\tau_1 = \epsilon^{1/2}\bar{t}$ . Then, in a neighbourhood  $U$  of the folded node the system is represented by

$$\begin{aligned} \dot{\bar{x}} &= \bar{y} - \bar{x}^2 \\ \dot{\bar{y}} &= \bar{z} - \bar{x} \\ \dot{\bar{z}} &= -\nu. \end{aligned}$$

In the following analysis, the bars will be omitted for readability. One important realisation is that the phase portraits for the rescaled system is topologically equivalent to the original normal form. Therefore, the mapping of solutions found in the blown up system to the original system is straightforward. ++++check if true++++ All the information needed to describe the dynamics near the fold point is now derived and therefore the next step in the analysis is the description of the SAOs. The SAOs in the folded node case are standard trajectories that follow a certain pattern. These patterns are, as discussed in Theorem 8.1, found by considering the eigenvalue ratio  $\mu$ . In the case of the folded node,  $\mu$  satisfies  $2k + 1 < \mu^{-1} < 2k + 3$ . Solving for  $k \in \mathbf{N}$ , then  $k$  is the number of secondary canards in the system as stated in Theorem 8.1. Furthermore,  $k$  corresponds to the number of twists the primary canard  $\gamma_s$  is performing around  $\gamma_w$ . A twist corresponds to a  $180^\circ$  rotation, see ?. It is important to note that  $\mu^{-1} \notin \mathbf{N}$  in order to conclude the number of secondary canards. If  $\mu^{-1} \in \mathbf{N}$  These SAOs are happening when trajectories get funneled into the region of the fold and contracted along the direction of  $S^a(++++?????+++)$ . For different values of  $\epsilon$ , the funnel gets narrower. For  $\epsilon \rightarrow 0$ , the maximum canard basically coincides with all of them... or something like that.... The number of SAOs an incoming trajectory undergoes depends on where the trajectory enters the fold region in the  $z$  plane. Different intervals of  $z$  can be defined in order to indicate for which values of  $z$  a certain amount of SAOs will be observed. The intervals are not 'clear cut', and a mix can happen ++??+++. The interval for the primary strong canard

is significantly larger, so the secondary canards close to it will have a higher amplitude (? reasoning right?) while the number of SAOs is smaller. As the number of SAOs increases, the amplitude of oscillations get smaller (contraction ?) and are not readily visible. The result about the width of the intervals is summed up in the following theorem.

**Theorem 9.2 (Width of Rotational Sectors)**

[Desroches et al. 2012] Consider system (58) and assume it has a folded-node singularity. At an  $O(1)$  distance from the fold curve, all secondary canards are in an  $O(\epsilon^{(1-\mu)/2})$  neighbourhood of the primary strong canard. Hence, the width of the rotational sectors  $I_i, 1 \leq i \leq k$ , is  $O(\epsilon^{(1-\mu)/2})$  and the width of sector  $I_{k+1}$  is  $O(1)$ .

++++++Maybe the actual pictures (2-3) would be a good idea+++++

++++++Return Mechanism+++++ As mentioned above, there are certain criteria that indicate the existence of a global return mechanism and therefore that MMOs can be observed. There are two theorems related to this issue, which are stated below. The first one is rather technical, stating the existence of the global return under certain circumstances, when the trajectory is in the rotational sector  $I_{k+1}$ , meaning, close to the weak primary canard and the  $k + 1$  number of SAOs, is hard to observe. Furthermore, as mentioned above, the width of the sector is much smaller than that of the primary canard, which is why the oscillations happen with fast speed, Therefore, the logical conclusion is to investigate whether a global return mechanism exists for the other  $I_i$ , for  $i \leq k$ . The existence of these MMOs is discussed in the second Theorem in this section. As introduced in the beginning of Section 9, the signatures of MMOs are represented in terms of the number of large amplitude oscillations  $L_1 L_2 \dots$  and the number of small amplitude oscillations  $s^1 s^2 \dots$ , and the conventional notation is  $L_1^{s^1} L_2^{s^2} \dots$ . In the case of the folded node, under the conditions of the theorems, we have a rather straightforward signature. The first theorem states the existence of the signature  $1^{k+1}$ , where  $L_1 = 1$  and  $s^1 = k + 1$ , and equivalently, the second theorem in this chapter discusses MMOs with signature  $1^i, i < k$ . The theorems are as follows. (++  $K + 1$  are maximal MMO signatures++) something about deltas too++++

**Theorem 9.3 (Generic  $1^{k+1}$  MMOs)**

[Desroches et al. 2012] Consider system (58) with the following assumptions:

1. Assume that  $0 < \epsilon \ll 1$  is sufficiently small,  $\epsilon^{1/2} \ll \mu$ , and  $k \in \mathbf{N}$  is such that  $2k + 1 < \mu^{-1} < 2k + 3$ .
2. The critical manifold  $S$  is (locally) a folded surface.
3. The corresponding reduced problem possesses a folded-node singularity.
4. There exists a candidate periodic orbit, which consists of fast fibres of the layer problem, a global return segment, and a segment on  $S^a$  within the funnel that starts at distance  $\delta$  from  $\bar{\gamma}_s$  (as measured at a distance  $O(1)$  away from the fold  $F$ ).
5. An appropriate transversality hypotheses is satisfied.

Then there exists a stable MMO with signature  $1^{k+1}$ .

**Theorem 9.4 (Stable MMOs with signature  $1^i$ )**

[Desroches et al. 2012] Suppose system (58) satisfies assumptions 1. - 4. of Theorem 9.3 and, the following additional assumption:

- For  $\delta = 0$ , the global return point is on the singular strong canard  $\bar{\gamma}_s$  and as  $\delta$  passes through zero the return point crosses  $\bar{\gamma}_s$  with nonzero speed.

Suppose now that  $\delta = O(\epsilon^{(1-\mu)/2}) > 0$ . Then, for sufficiently small  $0 < \epsilon \ll 1$  and  $k \in \mathbb{N}$  such that  $2k + 1 < \mu^{-1} < 2k + 3$ , the following holds. For each  $i, 1 \leq i \leq k$ , there exist subsectors  $\bar{I}_i \subset I_i$  with the corresponding distance intervals  $(\delta_i^-, \delta_i^+)$  of widths  $O(\epsilon^{(1-\mu)/2})$ , which have the property that if  $\delta \in (\delta_i^-, \delta_i^+)$ , then there exists a stable MMO with signature  $1^i$ .

++++++i think more talk about funnels and contractions would be good for this chapter++++++ all we need is the trajectory to go back into the funnel region. then we're good :)

### 9.3 Singular Hopf Bifurcation

In this section the folded saddle-node of type 2 and the saddle focus are considered for analysis. The folded saddle-node o type 2 occurs, when the parameters of the system coincide in such a way that an equilibrium of the full system and a fold point coincide. A saddle-node of type one refers to the case when only an equilibrium of the reduced system crosses a fold, without coinciding with a global equilibrium. If a saddle-node type 2 occurs for a specific parameter (also plural...), then a singular hopf bifurcation arises at  $O(\epsilon)$  away from the equilibrium. The equilibrium is focus if the eigenvalues corresponding to it are complex and a node if the eigenvalues are real.

**Definition 9.5. Singular Hopf Bifurcation**[Strogatz 2007](but also MMO)

A singular hopf bifurcation occurs at a certain parameter regime in the system which is  $O(\epsilon)$  away from a saddle-node of type 2. There, the eigenvalues of the system cross the imaginary axis, therefore they have a zero real part. Then small oscillations, called limit cycles occur in the system. There are two types of singular Hopf Bifurcation. The supercritical Hopf Bifurcation occurs when a stable limit cycle arises from an unstable equilibrium point, while the subcritical Hopf Bifurcation causes unstable limit cycles to appear around a stable equilibrium.

These different orbits caused by a singular Hopf Bifurcation are of interest, because they are SAOs of the fast-slow system in question. Therefore, in this chapter we will give an overview of the different SAOs arising from singular Hopf Bifurcations in different parameter regimes. The starting point of the analysis is the normal form considered for the folded node in section +++toms section++, which is then modified to a system that displays a singular Hopf Bifurcation and later on a system with a global return mechanism will be derived. The first transformation is achieved by adding higher-order terms to the  $z$  equation of system (++ toms normal form++). It then becomes

$$\begin{aligned}\epsilon \dot{x} &= y - x^2, \\ \dot{y} &= z - x \\ \dot{z} &= -\nu - ax - by - cz,\end{aligned}$$

which is the normal form for a singular Hopf Bifurcation. We then consider a coordinate transformation and time rescaling of the form

$$x = \epsilon^{1/2} \bar{x}, \quad y = \epsilon \bar{y}, \quad z = \epsilon^{1/2} \bar{z}, \quad t = \epsilon^{1/2} \bar{t}.$$

Then the system becomes

$$\bar{x}' = \bar{y} - \bar{x}^2, \tag{73}$$

$$\bar{y}' = \bar{z} - \bar{x}, \tag{74}$$

$$\bar{z}' = -\nu - \epsilon^{1/2} a \bar{x} - \epsilon b \bar{y} - \epsilon^{1/2} c \bar{z}. \tag{75}$$

This transformation can be seen, somewhat equivalently to Section 6.1, as a consideration of a small neighbourhood of the singular point. As described in Section 8, folded singularity is found by examining the critical manifold  $C = \{(x, y, z) : f := y - x^2 = 0\}$ . The conditions (56) are easily checked and satisfy:

$$\begin{aligned} f(p_*, \nu, \epsilon) &= y - x^2 = 0 \\ \Rightarrow y &= x^2 \\ \frac{\partial}{\partial x} f(p_*, \lambda, 0) &= -2x = 0, \\ \Rightarrow x &= 0 \\ \Rightarrow y &= 0 \\ \frac{\partial^2}{\partial x^2} f(p_*, \lambda, 0) &= -2 \neq 0, \\ D_{(y,z)} f(p_*, \lambda, 0) &= (1, 0) \end{aligned}$$

++++++Help!! Fold conditions do not work out....+ also no idea what the parameters are  $\nu, \epsilon$ ? is it going to zero....++++++ The folded singularity is found at  $p_* = (0, 0, z)$ , which makes the further analysis slightly more straightforward. The equilibria of the system are, such that  $p_0 = (x, x^2, x)$ , where  $x$  satisfies:

$$x = -\frac{1}{2\epsilon^{1/2}b} \left( (a + c) \pm \sqrt{(a + c)^2 - 4b\nu} \right), \quad (76)$$

and therefore there are two equilibria++is it correct that i have 2??++++ at

$$\begin{aligned} x_1 &= -\frac{a + c}{\epsilon^{1/2}b} + \frac{\nu}{\epsilon^{1/2}(a + c)} + \frac{b\nu^2}{\epsilon^{1/2}(a + c)^3} + \dots \\ x_2 &= \frac{\nu}{\epsilon^{1/2}(a + c)} + \frac{b\nu^2}{\epsilon^{1/2}(a + c)^3} + \dots, \end{aligned}$$

where a MacLaurin expansion for  $\sqrt{(a + c)^2 - 4b\nu}$  has been used. There exists a value for  $x$  depending on the parameters  $a, b, c$  and  $\nu$ , where a fold point intersects with the equilibrium. This is at  $x_1 = 0$  and  $x_2 = 0$ . Then, setting (76) to zero results in

$$\begin{aligned} x &= -\frac{1}{2\epsilon^{1/2}b} \left( (a + c) \pm \sqrt{(a + c)^2 - 4b\nu} \right) = 0 \\ \Rightarrow \nu &= -\frac{(a + c)^2 - (a + c)}{4b}. \end{aligned}$$

Therefore, the location of the singular equilibrium, depends on the parameter values for  $a, b, c$ .

Since  $a, b$  and  $c$  are all multiplied by a factor of  $\epsilon^{1/2}$  or  $\epsilon$  in system (73), we need  $\nu$  to be of  $O(\epsilon^{1/2})$  or smaller in order to observe a singular hopf bifurcation. If  $\nu = O(1)$ , then the factors of  $\epsilon$  in system (73) do not really contribute to the system and are merely a perturbation of the normal form (+++toms normal form+++). If  $\nu \leq O(\epsilon^{1/2})$ , then a singular hopf bifurcation occurs at a distance  $\nu = O(\epsilon)$  in parameter space away from the equilibrium. The eigenvalues of the system (73) can be found by considering the following Jacobian matrix associated to it:

$$J = \begin{bmatrix} 2x & 1 & 0 \\ -1 & 0 & 1 \\ -\epsilon^{1/2}a & -\epsilon b & -\epsilon^{1/2}c \end{bmatrix}. \quad (77)$$

Using a computer package, such as Maple, to solve for the eigenvalues confirms that there exist two complex eigenvalues for the equilibrium where  $x = 0$ . Since the eigenvalues of the system are complex, the equilibrium

is a saddle-focus, which has not been discussed in the analysis of canard trajectories. (+++++loop back to 3dim singularities and why we dont have canards)++++++ The research of the dynamics, and specifically MMOs, close to a singular Hopf Bifurcation is still ongoing. Here we only consider a few specific cases, where  $\nu$  is treated as the main parameter of interest. Furthermore, since the critical manifold in system (73) is in the shape of a quadratic function, by the geometrical nature of the problem, there is no global return mechanism for the system. Trajectories that leave the close proximity of the equilibrium do not return. In order to get MMOs, additionally to the SAOs a global return mechanism is needed. This is achieved by modifying system (73) by adding a cubic term to the  $x$  equation. This will change the shape of the critical manifold to an S shaped curve and therefore allow for a global return mechanism. The new system is then the following:

$$\begin{aligned}\epsilon \dot{x} &= y - x^2 - x^3, \\ \dot{y} &= z - x, \\ \dot{z} &= -\nu - ax - by - cz.\end{aligned}$$

The expected behaviour of the new system is now to display several SAOs close to the equilibrium, before completing a large amplitude oscillation. This LAO is necessarily of the form of a relaxation oscillation, because there is only one fast variable present in the system. This represents a constraint since the fast subsystem is one dimensional and therefore trajectories are restricted to be monotonic.

There are now many different types of MMOs present, depending on the parameter regimes. One example is that for small values of  $\nu$ , where  $\nu = O(\epsilon)$ , a stable periodic orbit  $\Gamma$  arises from the saddle-focus equilibrium. This orbit is tracing out SAOs close to the repelling sheet of the critical manifold, before completing a relaxation oscillation and returning to its starting point. However, other bifurcations can occur for these periodic orbits for different parameter regimes. These could be of the form of torus bifurcations or period-doubling. Then there is a possibilities of chaotic MMOs existing for these parameters. For decreasing values of  $\nu$  here, which is already  $O(\epsilon)$ , large amplitudes are getting smaller until the system only displays chaotic SAOs(++++++not sure if terminology works like this...++++)

Now it is of interest to consider specific parameter regimes for which the SAOs are constrained to the unstable manifold  $W^u(p_*)$ , which corresponds to the phase space surrounding the equilibrium  $p_*$ , while being backward asymptotic to it. For a supercritical Hopf Bifurcation we just observe the stable oscillation, as before. However, there is another type of bifurcation (++++WHY++++++) under certain conditions ( $W^u$  tangent to S)

## 10 Acknowledgements

Maple (specify release). Maplesoft, a division of Waterloo Maple Inc., Waterloo, Ontario.

## References

- Desroches, M., Guckenheimer, J., Krauskopf, B., Kuehn, C., Osinga, H. M. & Wechselberger, M. (2012), ‘Mixed-mode oscillations with multiple time scales’, *SIAM Rev.* **54**(2), 211–288.  
**URL:** <http://dx.doi.org/10.1137/100791233>
- Eckhaus, W. (1970), *Relaxation oscillations including a standard chase on French ducks*, Vol. 985, Springer, pp. 449–494.
- Festschrift, Broer, H., Krauskopf, B. & Vegter, G. (2001), ‘Global analysis of dynamical systems festschrift dedicated to floris takens for his 60th birthday’. Dedicated To Floris Takens.
- Hek, G. (2009), ‘Geometric singular perturbation theory in biological practice’, pp. 347–386.
- Krupa, M. & Szmolyan, P. (2001), ‘Extending geometric singular perturbation theory to nonhyperbolic points - fold and canard points in two dimensions’, *SIAM J. Math. Analysis* **33**(2), 286–314.
- Kuehn, C. (2015), *Multiple Time Scale Dynamics*, Vol. 191 of *Applied Mathematical Sciences*, Springer International Publishing, Cham.
- Mishchenko, E. (2012), *Differential Equations with Small Parameters and Relaxation Oscillations*, Mathematical Concepts and Methods in Science and Engineering, Springer US.  
**URL:** [https://books.google.co.uk/books?id=\\_UFZmQEACAAJ](https://books.google.co.uk/books?id=_UFZmQEACAAJ)
- Strogatz, S. (2007), *Nonlinear Dynamics And Chaos*, Studies in nonlinearity, Sarat Book House, chapter 7, p. 198.  
**URL:** <https://books.google.co.uk/books?id=PHmED2xxrE8C>
- Szmolyan, P. & Wechselberger, M. (2001), ‘Canards in  $r^3$ ’, *Journal of Differential Equations* **177**(2), 419 – 453.  
**URL:** <http://www.sciencedirect.com/science/article/pii/S002203960194001X>

## A Elements of Dynamical Systems

In this appendix we state some standard results from dynamical systems theory.

### A.1 Stable Manifold Theorem

Suppose  $\dot{x} = F(x)$  where  $x \in \mathbf{R}^n, F \in C^r(\mathbf{R}^n, \mathbf{R}^n)$  and has only hyperbolic fixed points (i.e. in the associated linearised system  $\dot{x} = Ax, A \in \mathbf{R}^n$  has no eigenvalues  $\lambda$  such that  $\text{Re}(\lambda) = 0$ ).

### A.2 Centre Manifold Theorem

### A.3 Implicit Function Theorem

### A.4 Hartman Grobman Theorem

DO we need this?

### A.5 Hopf Bifurcations

## B Theorems

#### Theorem B.1 (Krupa & Szmolyan (2001))

Assume that system (3.1) satisfies the defining non-degeneracy conditions (Equations 34 and 35) of a canard point. Assume that the solution  $x_0(t)$  of the reduced problem connects  $S_a$  to  $S_r$ . Then there exists  $\epsilon_0 > 0$  and a smooth function  $\lambda_c(\sqrt{\epsilon})$  defined on  $[0, \epsilon_0]$  such that for  $\epsilon \in (0, \epsilon_0)$  the following assertions hold:

—  $\pi(q_{a,\epsilon}) = q_{r,\epsilon}$  iff  $\lambda = \lambda_c(\sqrt{\epsilon})$ .

— The function  $\lambda_c$  has the expansion

$$\lambda_c(\sqrt{\epsilon}) = -\epsilon\left(\frac{a_1 + a_5}{2} + \frac{A}{8}\right) + O(\epsilon^{\frac{3}{2}}).$$

— The transition map  $\pi$  is defined only for  $\lambda$  in an interval around  $\lambda_c(\sqrt{\epsilon})$  of width  $O(\exp(-\frac{c}{\epsilon}))$  for some  $c > 0$ .

$$\frac{\partial}{\partial \lambda}(\pi(q_{a,\epsilon}) - q_{r,\epsilon})|_{\lambda=\lambda_c(\sqrt{\epsilon})} > 0$$

## C Numerical Simulation

Many figures in this document? were produced using MATLAB, for example: fig ++++++. In this appendix, we will give a brief tutorial on their production. Fast-slow systems like the ones studied here are a classic example of *stiff* ODEs<sup>a</sup>.

**Definition C.1** (Stiffness Ratio). Consider  $\dot{x} = F(x)$  where  $x \in \mathbf{R}^n, F \in C^r(\mathbf{R}^n, \mathbf{R}^n)$ . Let

$$x' = Ax, \quad A \in \mathbf{R}^{n \times n}$$

---

<sup>a</sup>Indeed, the MATLAB documentation for its stiff solver, `ode15s`, uses the Van Der Pol equation as it's example.

denote its linearisation. Suppose all the eigenvalues  $\lambda_j$  of  $A$  have negative real parts. Then the *stiffness ratio*,  $\mu$  is defined as

$$\mu := \frac{\max_j(\operatorname{Re}(\lambda_j))}{\min_j(\operatorname{Re}(\lambda_j))}$$

If  $\mu$  is large, the system is called *stiff*.

Stiffness is not a well-defined concept, it can be seen as a general term for a set of equations which are difficult to solve numerically to a high level of accuracy. Throughout this section we will consider the general problem above as an initial value problem.

$$\begin{cases} \dot{x} = F(x) \\ x(T_0) = x_0 \end{cases}$$

As before,  $x \in \mathbf{R}^n$  and  $F \in C^r(\mathbf{R}^n, \mathbf{R}^n)$ . To solve such a system numerically, time must be discretised. Using standard notation, let  $h$  be the time step between points on the solution. To differentiate between the continuous solution  $x(t)$  and the discretised solution, we denote the latter by  $x(t_j) = x_j$ . Here  $t_j = T_0 + jh$ . As a first example, consider the modified Euler method.

$$x(t_{n+1}) = x(t_n) + hF\left(x(t_n) + \frac{1}{2}F(x(t_n))\right)$$

Or, in the more compact notation,

$$x_{n+1} = x_n + hF\left(x_n + \frac{1}{2}F(x_n)\right)$$

This is a simple method and provides a starting point in considering error between true and numerical solutions.

The go-to ODE solver in MATLAB is `ode45`. This function uses the Dormand-Prince Runge-Kutta method, an explicit single-step formula. The Runge-Kutta method (RK4) is similar to the explicit Euler method in that it calculates the next point ( $x_{n+1}$ ) using only its current value ( $x_n$ ). Unlike the Euler method however, it yields much lower error by using a better approximation of the derivative at points in between  $x_n$  and  $x_{n+1}$  as opposed to only the derivative at the initial point. The Runge-Kutta method uses the following relation.

$$x_{n+1} = x_n + \frac{1}{6}h(k_1 + 2k_2 + 2k_3 + k_4)$$

where

$$\begin{aligned} k_1 &= F(x_n) \\ k_2 &= F\left(x_n + \frac{1}{2}hk_1\right) \\ k_3 &= F\left(x_n + \frac{1}{2}hk_2\right) \\ k_4 &= F(x_n + hk_3) \end{aligned}$$

The Runge-Kutta family of solvers are ubiquitous in numerical analysis, and most methods can be categorised as belonging to this set of methods. Even the simplest, the explicit Euler scheme, is a RK method. Note that `ode45` doesn't use RK4, it uses an adaptive method that repeats steps if the error in the step is too high. This produces an even more accurate solution without adding much computational cost.

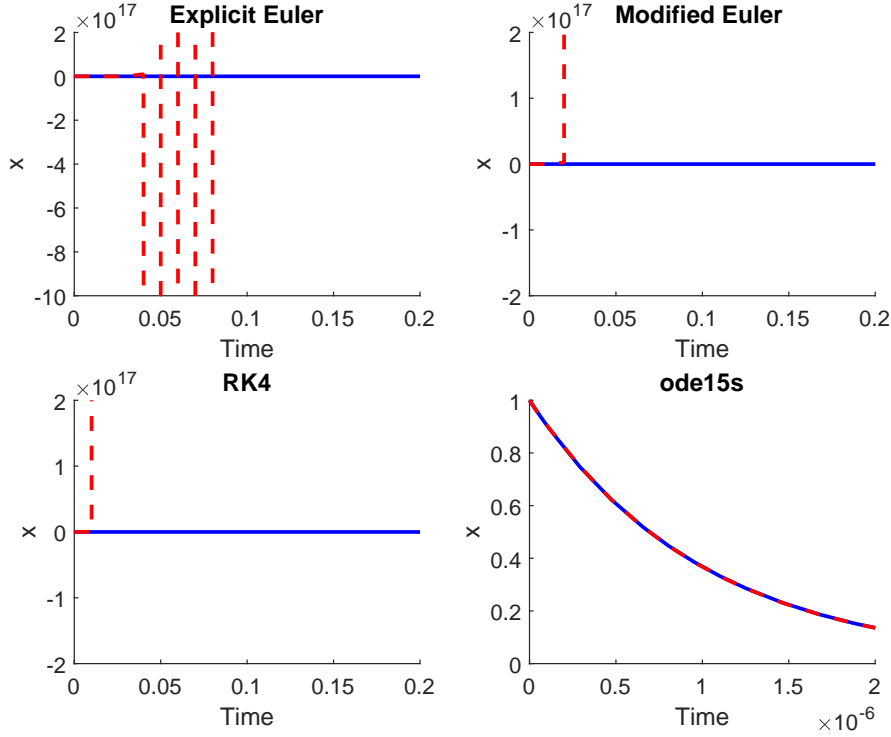


Figure 15: Comparison of stability of different numerical schemes applied to Equation 78. Blue solid line indicates analytic solution, dashed red indicates numeric solution using the scheme given in the plot title. Note the varying scales on the axes.

Let's look at the use of these various methods on the simplest fast-slow system.

$$\begin{cases} \begin{pmatrix} \dot{x} \\ \dot{y} \end{pmatrix} = \begin{pmatrix} -1/\epsilon & 0 \\ 0 & -1 \end{pmatrix} \begin{pmatrix} x \\ y \end{pmatrix} \\ (x(0), y(0)) = (x_0, y_0) \end{cases} \quad (78)$$

This system has an easy analytic solution,  $x(t) = x_0 \exp(-t/\epsilon)$ ,  $y(t) = y_0 \exp(-t)$ . For this reason it is a useful test system with which to analyse the convergence of numerical schemes. The stiffness ratio for this system is

$$\mu = \frac{\max_j(\operatorname{Re}(\lambda_j))}{\min_j(\operatorname{Re}(\lambda_j))} = \frac{1}{\epsilon}$$

The time separation,  $\epsilon \ll 1$  and so this system is very stiff. We thus expect explicit solvers to perform poorly.  
+++Explain about convergence here? Would be nice to do for modEuler and RK4 too+++.

The lack of stability of these algorithms in practice, even for very simple systems, clearly necessitates the introduction of alternative methods.

### C.1 Stiff Solvers

+++ode15s,ode23t,ode23s use, comparison of speed with ode45. Note difference between RK4.+++  
Test on RK4, mod-Euler and ode15s? Intro BDF? Check sec8 MMO.

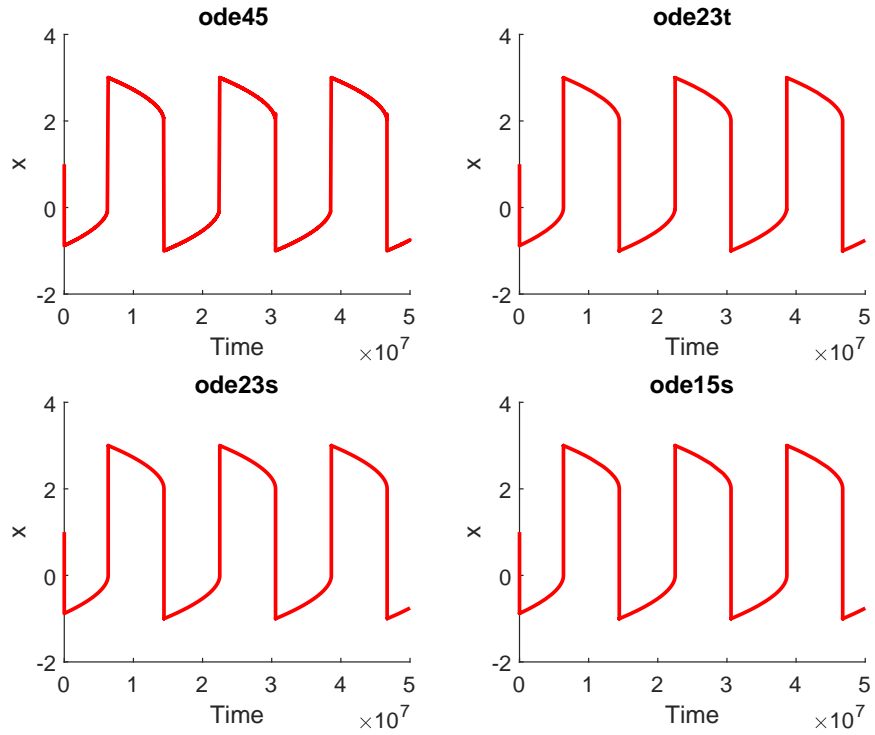


Figure 16: Comparison of stiff solvers for VDP. +++Note all get correct trajectory, what about speed?+++.

## D Dynamics in $K_2$